Eur. Phys. J. C (2012) 72:2012
DOI 10.1140/epjc/s10052-012-2012-3

THE EUROPEAN PHYSICAL JOURNAL C

Regular Article - Experimental Physics

Centrality dependence of dihadron correlations and azimuthal anisotropy harmonics in PbPb collisions at $\sqrt{s_{NN}} = 2.76$ TeV

The CMS Collaboration*
CERN, Geneva, Switzerland

Received: 20 January 2012 / Revised: 30 April 2012 / Published online: 30 May 2012

Abstract Measurements from the CMS experiment at the LHC of dihadron correlations for charged particles produced in PbPb collisions at a nucleon–nucleon centre-of-mass energy of 2.76 TeV are presented. The results are reported as a function of the particle transverse momenta (p_{T}) and collision centrality over a broad range in relative pseudorapidity ($\Delta\eta$) and the full range of relative azimuthal angle ($\Delta\phi$). The observed two-dimensional correlation structure in $\Delta\eta$ and $\Delta\phi$ is characterised by a narrow peak at $(\Delta\eta, \Delta\phi) \approx (0, 0)$ from jet-like correlations and a long-range structure that persists up to at least $|\Delta\eta| = 4$. An enhancement of the magnitude of the short-range jet peak is observed with increasing centrality, especially for particles of p_{T} around 1–2 GeV/c. The long-range azimuthal dihadron correlations are extensively studied using a Fourier decomposition analysis. The extracted Fourier coefficients are found to factorise into a product of single-particle azimuthal anisotropies up to $p_{\mathrm{T}} \approx 3$–3.5 GeV/c for at least one particle from each pair, except for the second-order harmonics in the most central PbPb events. Various orders of the single-particle azimuthal anisotropy harmonics are extracted for associated particle p_{T} of 1–3 GeV/c, as a function of the trigger particle p_{T} up to 20 GeV/c and over the full centrality range.

1 Introduction

Measurements of dihadron correlations are a well established technique for studying the properties of particle production in the high density medium created in heavy ion collisions. Early results from PbPb collisions at the Large Hadron Collider (LHC) [1, 2] extended these studies into a regime of much higher beam energies as compared to those from the Relativistic Heavy Ion Collider (RHIC) [3–10]. These results complement other LHC measurements of medium properties, including a large deficit of charged particles at high-p_{T} [11] and the observations of an enhanced fraction of dijets with very asymmetric energies [12, 13].

The Compact Muon Solenoid (CMS) experiment at the LHC has studied dihadron correlations over a broad range of relative azimuthal angles ($|\Delta\phi|$) and pseudorapidity ($|\Delta\eta|$, where $\eta = -\ln[\tan(\theta/2)]$ and θ is the polar angle relative to the counterclockwise beam axis) in the most central PbPb collisions at a nucleon–nucleon centre-of-mass energy ($\sqrt{s_{NN}}$) of 2.76 TeV [1]. Concentrating on large $|\Delta\eta|$, previous measurements at RHIC established some of the properties of the so-called "ridge" [4, 6, 9], an enhancement of pairs with $|\Delta\phi| \approx 0$. While a variety of theoretical models have been proposed to interpret the ridge phenomena as a consequence of jet-medium interactions [14–19], recent theoretical developments indicate that, because of event-by-event fluctuations in the initial shape of the interacting region, sizeable higher-order hydrodynamic flow terms could also be induced, e.g., triangular flow [20–28]. The triangular flow effect will contribute to the dihadron correlations in the form of a $\cos(3\Delta\phi)$ component, which also gives a maximum near-side correlation at $\Delta\phi \approx 0$, similarly to the elliptic flow contribution. It has been proposed that by taking into account various higher-order terms, the ridge structure could be described entirely by hydrodynamic flow effects [23]. To investigate this possibility, a Fourier decomposition of the CMS data at large $|\Delta\eta|$ was performed, finding a strong dependence on p_{T} [1]. Similar results, although with a smaller $|\Delta\eta|$ gap, have been reported by ALICE [2, 29]. The observations by CMS of a ridge-like structure in very high multiplicity proton-proton (pp) collisions at a centre-of-mass energy of 7 TeV [30], where no medium effect is expected, may also challenge the interpretations of these long-range correlations.

This paper, expanding on previous CMS results [1], presents dihadron correlation measurements from PbPb col-

* e-mail: cms-publication-committee-chair@cern.ch

lisions at $\sqrt{s_{NN}} = 2.76$ TeV acquired in 2010, for all collision centralities and over a broader range of hadron p_T. As in Refs. [1, 30], the yield of particles (binned in p_T) associated with a trigger particle (also binned in p_T) is extracted as a function of their relative pseudorapidity and azimuthal angle. Such a study of hadron pairs in either the same or different p_T ranges can reveal important information about the production of particles and their propagation through the medium. A Fourier decomposition technique is used to quantify the long-range azimuthal correlations. The potential connection between the extracted Fourier coefficients from the correlation data and the azimuthal anisotropy harmonics for single particles is investigated. This measurement provides a comprehensive examination of the centrality and transverse momentum ($1 < p_T < 20$ GeV/c) dependencies of the short-range ($|\Delta\eta| < 1$) and long-range ($2 < |\Delta\eta| < 4$) dihadron correlations in PbPb collisions at LHC energies, as well as the relationship between these two-particle correlations and single-particle angular distributions. These results provide extensive input to the interpretation of these observables in terms of broad theoretical concepts such as hydrodynamic flow and quantitative models of particle production and propagation in the high-density medium.

The detector, the event selection and the extraction of the correlation functions are described in Sects. 2 and 3, while the extracted results are described in Sects. 4 and 5.

2 CMS detector

The ability of the CMS detector (all components of which are described in Ref. [31]) to extract the properties of charged particles over a large solid angle is particularly important in the study of dihadron correlations. This study is based primarily on data from the inner tracker contained within the 3.8 T axial magnetic field of the large superconducting solenoid. The tracker consists of silicon pixel and strip detectors. The former includes 1 440 modules arranged in 3 layers, while the latter consists of 15 148 modules arranged in 10 (11) layers in the barrel (endcap) region. The trajectories of charged particles can be reconstructed for $p_T > 100$ MeV/c and within $|\eta| < 2.5$.

The field volume of the solenoid also contains crystal electromagnetic and brass/scintillator hadron calorimeters. Although not included in the present results, muons are detected using gas-ionisation counters embedded in the steel return yoke. In addition to these components in and around the barrel and endcap of the solenoid, CMS also has extensive forward calorimetry. In the right-handed coordinate system used by CMS, the x-, y-, and z-axes are aligned with the radius of the LHC ring, the vertical direction, and the counterclockwise beam direction, respectively, with the origin located at the centre of the nominal interaction region.

For PbPb collisions, the primary minimum-bias trigger uses signals from either the beam scintillator counters (BSC, $3.23 < |\eta| < 4.65$) or the steel/quartz-fibre Cherenkov forward hadron calorimeters (HF, $2.9 < |\eta| < 5.2$). Coincident signals from detectors located at both ends of the detector (i.e., a pair of BSC or a pair of HF modules) are required. Events due to noise, cosmic-ray muons, double-firing triggers, and beam backgrounds are suppressed by further requiring the presence of colliding beam bunches. The fraction of inelastic hadronic PbPb collisions accepted by this primary trigger is (97 ± 3) % [13].

3 Data and analysis

The procedure used in the present analysis follows that described in the previous CMS correlation paper [1]. Offline event selection requires a reconstructed vertex with at least two tracks (i.e., at least one pair of charged particles). This vertex must be within 15 cm along the beam axis relative to the centre of the nominal collision region and within 0.02 cm in the transverse plane relative to the average position of all vertices in a given data sample. In addition, various background events (for example beam-gas and beam-halo collisions, cosmic muons, and large-impact-parameter electromagnetic collisions) are suppressed by requiring at least three signals in the HF calorimeters at both positive and negative η, with at least 3 GeVof energy in each signal.

The analysis is based on a data sample of PbPb collisions corresponding to an integrated luminosity of approximately 3.9 μb^{-1} [32, 33], which contains 30 million minimum-bias collisions after all event selections are applied. The pp data at $\sqrt{s} = 2.76$ TeV, the reference for comparison to the PbPb data, were collected during a short low-energy LHC run at the end of March 2011. Minimum-bias-triggered pp events corresponding to an integrated luminosity of 520 μb^{-1} are selected for this analysis.

The energy released in the collisions is related to the centrality of the heavy ion interactions, i.e., the geometrical overlap of the incoming nuclei. The event centrality is defined as the fraction of the total cross section, starting at 0 % with the most central collisions (i.e., smallest impact parameter). This fraction is determined from the distribution of total energy measured in both HF calorimeters.

The event centrality can be correlated with the total number of nucleons in the two Pb nuclei that experienced at least one inelastic collision, N_{part}. The average values of N_{part} for the various centrality bins used in this analysis are given in Table 1. The N_{part} values are obtained using a Glauber Monte Carlo (MC) simulation [34, 35] with the same parameters as in Ref. [13]. These calculations are translated into reconstructed centrality bins using correlations between N_{part} and the measured total energy in the HF calorimeters,

Table 1 Average N_{part} values for each PbPb centrality range used in this paper. The values are obtained using a Glauber MC simulation with the same parameters as in Ref. [13]

Centrality	0–5 %	5–10 %	10–15 %	15–20 %	20–25 %	25–30 %
$\langle N_{\text{part}} \rangle$	381 ± 2	329 ± 3	283 ± 3	240 ± 3	203 ± 3	171 ± 3
Centrality	30–35 %	35–40 %	40–50 %	50–60 %	60–70 %	70–80 %
$\langle N_{\text{part}} \rangle$	142 ± 3	117 ± 3	86.2 ± 2.8	53.5 ± 2.5	30.5 ± 1.8	15.7 ± 1.1

obtained from fully simulated MC events. The systematic uncertainties on the N_{part} values in Table 1 are derived from propagation of the uncertainties in the parameters of the Glauber model. More details on the determination of centrality and N_{part} can be found in Refs. [13, 36, 37].

The reconstruction of charged particles in PbPb collisions is based on signals in the silicon pixel and strip detectors, similarly to the reconstruction for pp collisions [38]. However, a number of settings are adjusted to cope with the challenges presented by the much higher signal density in central PbPb collisions. A set of tight quality selections are imposed on the collection of fully reconstructed tracks to minimise the contamination from misidentified tracks. These include requirements of at least 13 signals on the track, a relative momentum uncertainty of less than 5 %, a normalised χ^2 of less than 0.15 times the number of signals, and transverse and longitudinal impact parameters of less than three times the sum in quadrature of the uncertainties on the impact parameter and the primary vertex position. Studies with simulated MC events show that the combined geometrical acceptance and reconstruction efficiency for the primary-track reconstruction reaches about 60 % for the 0–5 % most central PbPb collisions at $p_{\text{T}} > 2$ GeV/c over the full CMS tracker acceptance ($|\eta| < 2.4$) and 66 % for $|\eta| < 1.0$. The fraction of misidentified tracks is about 1–2 % for $|\eta| < 1.0$, but increases to 10 % at $|\eta| \approx 2.4$ for the 5 % most central PbPb collisions. For the peripheral PbPb events (70–80 %), the overall tracking efficiency improves by up to 5 %, with a much lower fraction of misidentified tracks.

The analysis of dihadron angular correlations in this paper follows exactly the procedure established in Ref. [1]. Any charged particle associated with the primary vertex and in the range $|\eta| < 2.4$ can be used as a trigger particle. A variety of bins of trigger transverse momentum, denoted by $p_{\text{T}}^{\text{trig}}$, are considered. There can be more than one such trigger particle in a single event and their total multiplicity in a particular data sample is denoted by N_{trig}. Within each event, every trigger particle is then paired with all of the remaining particles (again within $|\eta| < 2.4$). As for the trigger particles, these associated particles are binned in transverse momentum ($p_{\text{T}}^{\text{assoc}}$). The differential yield of associated particles per trigger particle is given by

$$\frac{1}{N_{\text{trig}}} \frac{\mathrm{d}^2 N^{\text{pair}}}{\mathrm{d}\Delta\eta\, \mathrm{d}\Delta\phi} = B(0,0) \times \frac{S(\Delta\eta, \Delta\phi)}{B(\Delta\eta, \Delta\phi)}, \tag{1}$$

where N^{pair} is the total number of correlated hadron pairs. The functions $S(\Delta\eta, \Delta\phi)$ and $B(\Delta\eta, \Delta\phi)$ are called the signal and background distributions, respectively. The value of the latter at $\Delta\eta = 0$ and $\Delta\phi = 0$ ($B(0,0)$) is a normalisation factor.

The signal distribution is the per-trigger-particle yield of pairs found in the same event,

$$S(\Delta\eta, \Delta\phi) = \frac{1}{N_{\text{trig}}} \frac{\mathrm{d}^2 N^{\text{same}}}{\mathrm{d}\Delta\eta\, \mathrm{d}\Delta\phi}, \tag{2}$$

where N^{same} is the number of such pairs within a $(\Delta\eta,\Delta\phi)$ bin. The background distribution is found using a mixed-event technique, wherein trigger particles from one event are combined (mixed) with all of the associated particles from a different event. In the analysis, associated particles from 10 randomly chosen events are used. The result is given by

$$B(\Delta\eta, \Delta\phi) = \frac{1}{N_{\text{trig}}} \frac{\mathrm{d}^2 N^{\text{mix}}}{\mathrm{d}\Delta\eta\, \mathrm{d}\Delta\phi}, \tag{3}$$

where N^{mix} denotes the number of mixed-event pairs. This background distribution represents the expected correlation if the only effects present were random combinatorics and pair-acceptance.

The value of $B(\Delta\eta, \Delta\phi)$ at $\Delta\eta = 0$ and $\Delta\phi = 0$ (with a bin width of 0.3 in $\Delta\eta$ and $\pi/16$ in $\Delta\phi$) is used to find the normalisation factor $B(0,0)$. In this case, the two particles have the maximum possible geometric pair acceptance since they are travelling in essentially the same direction. The effect of two tracks merging into a single reconstructed track is negligible. The extent to which the background distribution at larger angular separation is smaller than this value (more specifically the ratio $B(0,0)/B(\Delta\eta, \Delta\phi)$) can be used to determine the pair acceptance correction factor. Multiplying the signal distribution by this ratio gives the acceptance-corrected per-trigger-particle associated yield. Since the distributions should, in principle, be symmetric, the statistical precision is maximised by filling only one quadrant using the absolute values of $\Delta\eta$ and $\Delta\phi$. For illustration purposes only (for example, see Fig. 1), the other three quadrants are filled by reflection, giving distributions that are symmetric about $(\Delta\eta, \Delta\phi) = (0,0)$ by construction. The pair acceptance decreases rapidly with $\Delta\eta$ and so, to avoid large fluctuations

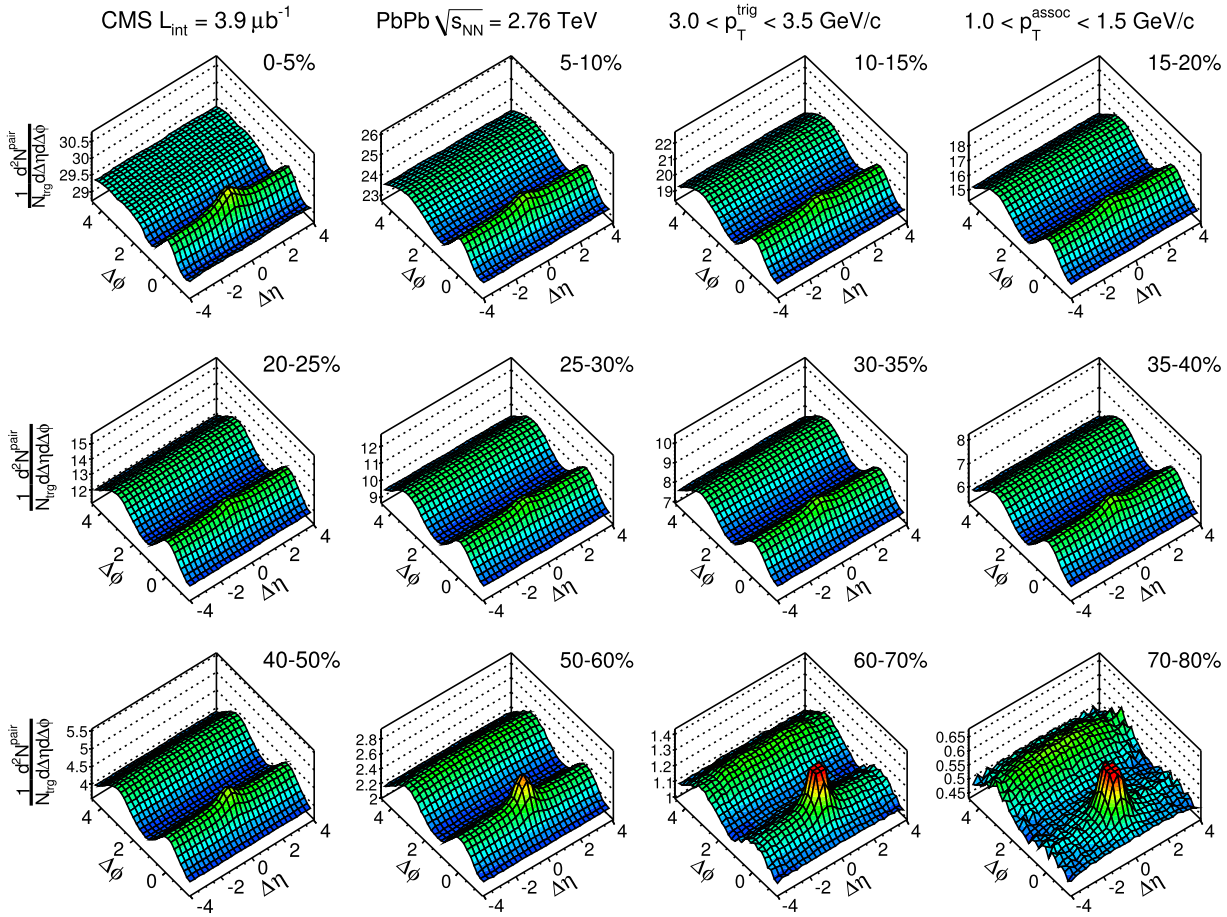

Fig. 1 Two-dimensional (2D) per-trigger-particle associated yield of charged hadrons as a function of $|\Delta\eta|$ and $|\Delta\phi|$ for $3 < p_{\mathrm{T}}^{\mathrm{trig}} < 3.5$ GeV/c and $1 < p_{\mathrm{T}}^{\mathrm{assoc}} < 1.5$ GeV/c, for twelve centrality ranges of PbPb collisions at $\sqrt{s_{NN}} = 2.76$ TeV. The near-side peak is truncated in the two most peripheral distributions to better display the surrounding structure

due to statistical limitations, the distributions are truncated at $|\Delta\eta| = 4$. The analysis is performed in twelve centrality classes of PbPb collisions ranging from the most central 0–5 % to the most peripheral 70–80 %. Within each centrality range, the yield described in Eq. (1) is calculated in 0.5 cm wide bins of the vertex position (z_{vtx}) along the beam direction and then averaged over the range $|z_{\mathrm{vtx}}| < 15$ cm.

When filling the signal and background distributions, each pair is weighted by the product of correction factors for the two particles. These factors are the inverse of an efficiency that is a function of each particle's pseudorapidity and transverse momentum,

$$\varepsilon_{\mathrm{trk}}(\eta, p_{\mathrm{T}}) = \frac{A(\eta, p_{\mathrm{T}})E(\eta, p_{\mathrm{T}})}{1 - F(\eta, p_{\mathrm{T}})}, \tag{4}$$

where $A(\eta, p_{\mathrm{T}})$ is the geometrical acceptance, $E(\eta, p_{\mathrm{T}})$ is the reconstruction efficiency, and $F(\eta, p_{\mathrm{T}})$ is the fraction of misidentified tracks. The effect of this weighting factor only changes the overall scale but not the shape of the associated yield distribution, which is determined by the signal-to-background ratio.

As described in Ref. [1], the track-weighting procedure is tested using MC events generated with HYDJET [39] (version 1.6) propagated through a full detector simulation. The tracking efficiencies themselves are checked using simulated tracks embedded into actual data events. Systematic uncertainties due to variations of the track reconstruction efficiency as a function of vertex location and also the procedure used to generate the background events are evaluated. The individual contributions are added in quadrature to find the final systematic uncertainties of 7.3–7.6 %.

4 Correlation functions and near-side yields

The two-dimensional (2D) per-trigger-particle associated yield distribution of charged hadrons as a function of $|\Delta\eta|$ and $|\Delta\phi|$ is measured for each $p_{\mathrm{T}}^{\mathrm{trig}}$ and $p_{\mathrm{T}}^{\mathrm{assoc}}$ interval, and in different centrality classes of PbPb collisions. An exam-

ple for trigger particles with $3 < p_{\mathrm{T}}^{\mathrm{trig}} < 3.5$ GeV/c and associated particles with $1 < p_{\mathrm{T}}^{\mathrm{assoc}} < 1.5$ GeV/c is shown in Fig. 1, for centralities ranging from the 0–5 % most central collisions, to the most peripheral (70–80 %) events. The 2D correlations are rich in structure, and evolve with centrality. The $p_{\mathrm{T}}^{\mathrm{trig}}$ and $p_{\mathrm{T}}^{\mathrm{assoc}}$ ranges shown in this figure were chosen as an example because they demonstrate a good balance of the following features. For the most central PbPb collisions, a clear and significant ridge-like structure mostly flat in $\Delta\eta$, and extending to the limit of $|\Delta\eta| = 4$, is observed at $\Delta\phi \approx 0$. At mid-peripheral events, a pronounced $\cos(2\Delta\phi)$ component emerges, originating predominantly from elliptic flow [10]. Lastly, in the most peripheral collisions, the near-side ridge structure has largely diminished, while the away-side back-to-back jet correlations can be clearly seen at $\Delta\phi \approx \pi$, but spread out in $\Delta\eta$.

As was done in Ref. [1], to quantitatively examine the features of short-range and long-range azimuthal correlations, one-dimensional (1D) $\Delta\phi$ correlation functions are calculated by averaging the 2D distributions over a limited region in $\Delta\eta$ from $\Delta\eta_{\mathrm{min}}$ to $\Delta\eta_{\mathrm{max}}$:

$$\frac{1}{N_{\mathrm{trig}}}\frac{\mathrm{d}N^{\mathrm{pair}}}{\mathrm{d}\Delta\phi} = \frac{1}{\Delta\eta_{\mathrm{max}} - \Delta\eta_{\mathrm{min}}}\int_{\Delta\eta_{\mathrm{min}}}^{\Delta\eta_{\mathrm{max}}} \frac{1}{N_{\mathrm{trig}}}\frac{\mathrm{d}^2N^{\mathrm{pair}}}{\mathrm{d}\Delta\eta\,\mathrm{d}\Delta\phi}\mathrm{d}\Delta\eta. \quad (5)$$

The results of extracting the 1D $\Delta\phi$ correlations in the short-range ($0 < |\Delta\eta| < 1$) and long-range ($2 < |\Delta\eta| < 4$) regions are shown in Fig. 2. The associated yield distribution per trigger particle is extracted for the same $p_{\mathrm{T}}^{\mathrm{trig}}$ and $p_{\mathrm{T}}^{\mathrm{assoc}}$ ranges as in Fig. 1.

In order to study the short-range $\Delta\phi$ correlations in the absence of the flat background in $\Delta\eta$, the 1D $\Delta\phi$ distribution in the long-range region is subtracted from that in the short-range region. The resulting difference of the distributions is shown in Fig. 3. The near-side peak ($\Delta\phi \approx 0$) represents mainly the correlations from jet fragmentation,

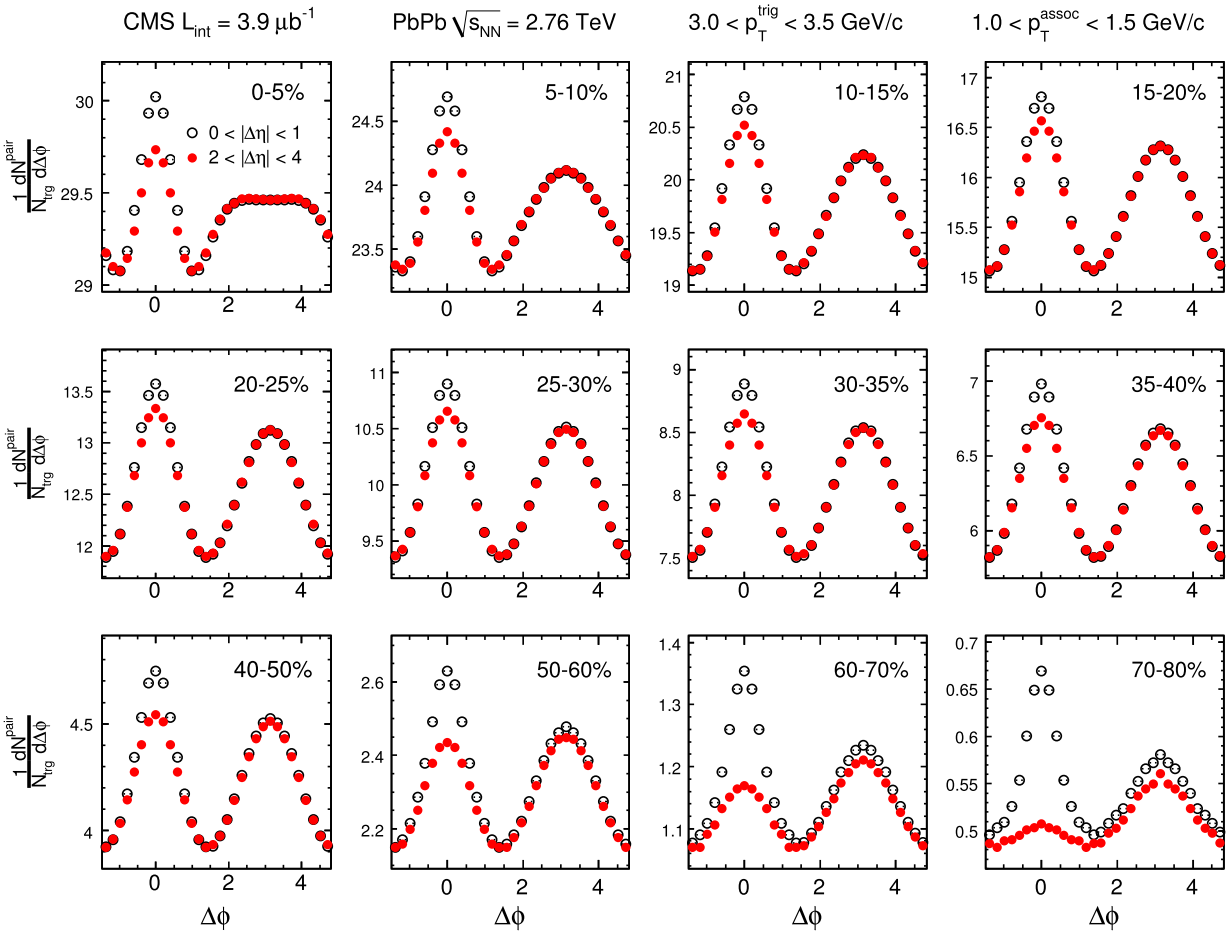

Fig. 2 Short-range ($0 < |\Delta\eta| < 1$, *open circles*) and long-range ($2 < |\Delta\eta| < 4$, *red closed circles*) per-trigger-particle associated yields of charged hadrons as a function of $|\Delta\phi|$ for $3 < p_{\mathrm{T}}^{\mathrm{trig}} < 3.5$ GeV/c and $1 < p_{\mathrm{T}}^{\mathrm{assoc}} < 1.5$ GeV/c, for twelve centrality ranges of PbPb collisions at $\sqrt{s_{NN}} = 2.76$ TeV. The statistical *error bars* are smaller than the marker size. The systematic uncertainties of 7.6 % for all data points in the short-range region and 7.3 % for all data points in the long-range region are not shown in the plots

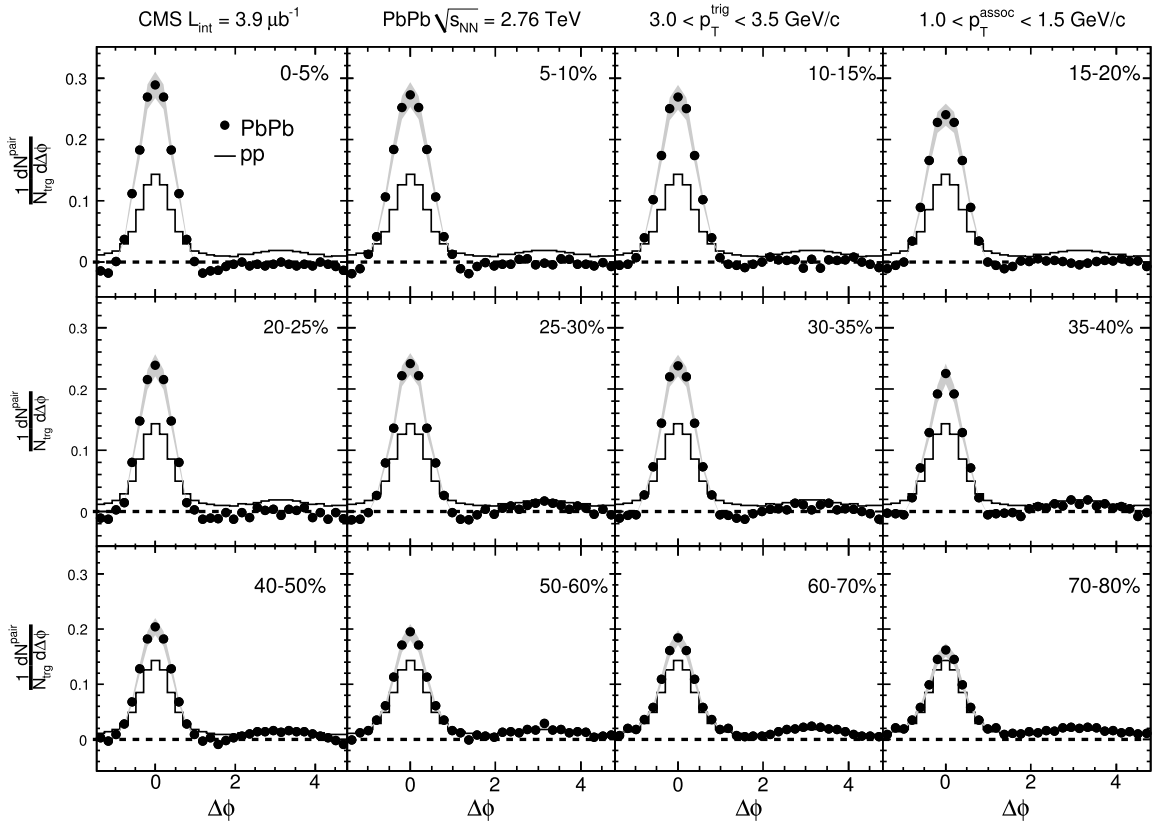

Fig. 3 The difference between short-range ($0 < |\Delta\eta| < 1$) and long-range ($2 < |\Delta\eta| < 4$) per-trigger-particle associated yields of charged hadrons as a function of $|\Delta\phi|$ for $3 < p_{\mathrm{T}}^{\mathrm{trig}} < 3.5$ GeV/c and $1 < p_{\mathrm{T}}^{\mathrm{assoc}} < 1.5$ GeV/c, for twelve centrality ranges of PbPb collisions at $\sqrt{s_{NN}} = 2.76$ TeV. The statistical *error bars* are smaller than the marker size. The *grey bands* denote the systematic uncertainties. The pp result is superimposed in all panels, for reference purposes

whereas the away-side region ($\Delta\phi \approx \pi$) is mostly flat and close to zero due to the weak $\Delta\eta$ dependence of the away-side jet peak. A comparison to the pp data at $\sqrt{s} = 2.76$ TeV is also presented, showing a similar structure to that in the very peripheral 70–80 % PbPb data. However, the magnitude of the near-side peak is significantly enhanced in the most central PbPb collisions as compared to pp. Most of the systematic uncertainties manifest themselves as an overall change in the scale of the correlation functions, with little dependence on $\Delta\phi$ and $\Delta\eta$. Therefore, they largely cancel when the difference between the short-range and long-range regions is taken.

The strengths of the near-side peak and away-side region in the $|\Delta\phi|$ distributions from Fig. 3 can be quantified by integrating over the two $|\Delta\phi|$ ranges separated by the minimum position of the distribution. This position is chosen as $|\Delta\phi| = 1.18$, the average of the minima between the near side and away side over all centralities. This choice of integration range introduces an additional systematic uncertainty in the integrated associated yields. The effect of choosing different minima for integration ranges changes the overall yield by an absolute amount of at most 0.007. Similar shifts are calculated for each data point, then added as an absolute value in quadrature to the other systematic uncertainties.

Figure 4 shows the integrated associated yields of the near-side peak and away-side regions as a function of N_{part} in PbPb collisions at $\sqrt{s_{NN}} = 2.76$ TeV, requiring $3 < p_{\mathrm{T}}^{\mathrm{trig}} < 3.5$ GeV/c, for four different intervals of $p_{\mathrm{T}}^{\mathrm{assoc}}$ (1–1.5, 1.5–2, 2–2.5, and 2.5–3 GeV/c). The grey bands represent the systematic uncertainties. For easier visual comparison between the most central PbPb results and the values one would expect from a trivial extrapolation of the pp results, the latter are also represented using horizontal lines covering the full N_{part} range. The yield of the near-side peak increases by a factor of 1.7 in going from the very peripheral 70–80 % to the most central 0–5 % PbPb events, for the lowest $p_{\mathrm{T}}^{\mathrm{assoc}}$ interval of 1–1.5 GeV/c. As $p_{\mathrm{T}}^{\mathrm{assoc}}$ increases, the centrality dependence of the near-side yield becomes less prominent. An increase by a factor of only 1.3 is observed for the highest $p_{\mathrm{T}}^{\mathrm{assoc}}$ interval of 2.5–3 GeV/c. This is of particular interest because at RHIC energies for $p_{\mathrm{T}}^{\mathrm{assoc}}$ down to

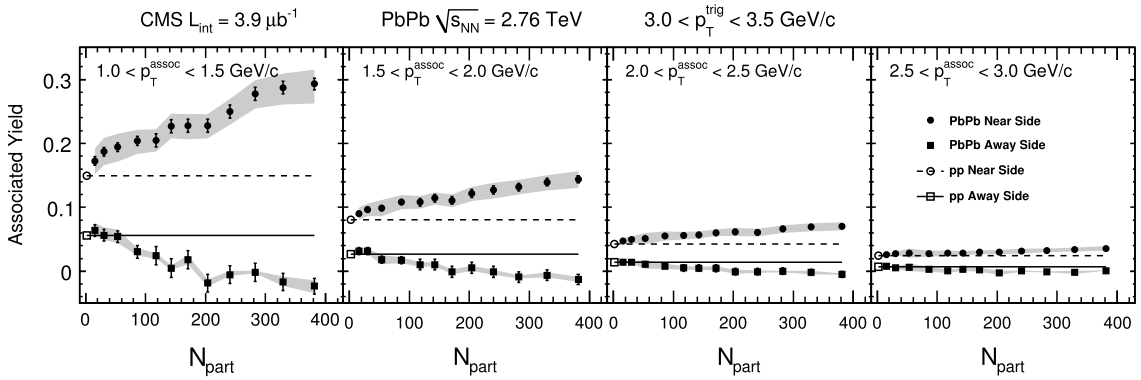

Fig. 4 The integrated associated yields of the near-side peak ($|\Delta\phi| < 1.18$) and away-side region ($|\Delta\phi| > 1.18$), requiring $3 < p_{\mathrm{T}}^{\mathrm{trig}} < 3.5$ GeV/c for four different intervals of $p_{\mathrm{T}}^{\mathrm{assoc}}$, as a function of N_{part} in PbPb collisions at $\sqrt{s_{NN}} = 2.76$ TeV. The *error bars* correspond to statistical uncertainties only. The *grey bands* denote the systematic uncertainties. The *lines* represent the pp results ($N_{\mathrm{part}} = 2$) superimposed over the full range of N_{part} values

2 GeV/c and similar $p_{\mathrm{T}}^{\mathrm{trig}}$ ranges and methodology, although for a lower density system (AuAu at $\sqrt{s_{NN}} = 0.2$ TeV), there is almost no centrality dependence observed [40]. On both near and away sides, the yield in PbPb matches that in pp for the most peripheral events. On the away side, the yield in PbPb decreases with centrality, becoming negative for the most central events. Variations in the event-mixing procedure can cause large fluctuations but only at the very edge of the acceptance around $|\Delta\eta| = 4.8$. However, the correlation function is only studied up to $|\Delta\eta| < 4$ in this paper so these fluctuations do not affect the results. The negative values of the yields in Fig. 4 are caused by a slightly concave structure on the away-side region ($1.18 < |\Delta\phi| < \pi$), i.e. the yields near $|\Delta\eta| \approx 0$ are smaller than those at higher $|\Delta\eta|$. The effect is more prominent for central PbPb events. However, this concavity is seen only for $|\Delta\eta| < 2$. Beyond that region, the $\Delta\eta$ distribution is found to be largely flat up to $|\Delta\eta| = 4$. Similar behaviour was also observed at RHIC for AuAu collisions at $\sqrt{s_{NN}} = 200$ GeV [41]. This deviation from pp may be related to the jet quenching phenomena, which leads to a modification in the back-to-back jet correlations in PbPb. Any effect that modifies the kinematics of dijet production could also result in a modification of away-side distributions in $\Delta\eta$. Additionally, any slight dependence of the flow effect on η could also play a role. More detailed theoretical models will be required to fully understand the origin of this small effect.

5 Fourier decomposition analysis of the PbPb data

The first Fourier decomposition analysis of long-range dihadron azimuthal correlations for PbPb collisions at $\sqrt{s_{NN}} = 2.76$ TeV was presented in Ref. [1]. This analysis was motivated by the goal of determining whether the long-range ridge effect was caused by higher-order hydrodynamic flow harmonics induced by the initial geometric fluctuations. This decomposition involves fitting the 1D $\Delta\phi$-projected distribution for $2 < |\Delta\eta| < 4$ (to avoid the jet peak) with a Fourier series given by

$$\frac{1}{N_{\mathrm{trig}}}\frac{\mathrm{d}N^{\mathrm{pair}}}{\mathrm{d}\Delta\phi} = \frac{N_{\mathrm{assoc}}}{2\pi}\left\{1 + \sum_{n=1}^{N_{\mathrm{max}}} 2V_{n\Delta}\cos(n\Delta\phi)\right\}, \tag{6}$$

where $V_{n\Delta}$ are the Fourier coefficients and N_{assoc} represents the total number of hadron pairs per trigger particle for the given $|\Delta\eta|$ range and ($p_{\mathrm{T}}^{\mathrm{trig}}$, $p_{\mathrm{T}}^{\mathrm{assoc}}$) bin. The first five Fourier terms ($N_{\mathrm{max}} = 5$) are included in both the current fits and those in Ref. [1]. In this paper, the analysis of the Fourier decomposition is extended to the full centrality range, and is performed as a function of both $p_{\mathrm{T}}^{\mathrm{trig}}$ and $p_{\mathrm{T}}^{\mathrm{assoc}}$.

The Fourier decomposition results have several systematic uncertainties. Because the tracking-correction-related systematic uncertainties only change the overall scale of the correlation functions, instead of the shape, they have only a ±0.8 % uncertainty on the extracted Fourier coefficients ($V_{n\Delta}$), largely independent of n and collision centrality. In addition, the results are insensitive to looser or tighter track selections to within ±0.5 %. By comparing the Fourier coefficients derived for two different z_{vtx} ranges, $|z_{\mathrm{vtx}}| < 15$ cm and $|z_{\mathrm{vtx}}| < 5$ cm, the systematic uncertainties due to the dependence on the vertex position are estimated to be less than ±0.5 %. Variations from the finite bin width of the $\Delta\phi$ histograms contribute the largest systematic uncertainty to the analysis, especially for the higher-order components, which are more sensitive to the fine structure of the distributions. Reducing the binning of the $\Delta\phi$ histograms by factors of 2, 4, and 8, the extracted Fourier coefficients vary by ±0.3–2.2 %. The effect of including additional higher-order Fourier terms in the fit using Eq. (6) results in changes of at most ±1.0 % (for $n = 5$), with Fourier terms up to $n = 10$

included ($N_{\max} = 10$). The values of additional higher-order Fourier terms included in the fit are all consistent with zero.

Table 2 summarises the different sources of uncertainty for the first five Fourier coefficients. These uncertainties are added in quadrature to obtain the total systematic uncertainties, also given in Table 2.

The fitted Fourier coefficients ($V_{n\Delta}$) up to $n = 5$, for two representative low-$p_{\mathrm{T}}^{\mathrm{trig}}$ ranges of $1 < p_{\mathrm{T}}^{\mathrm{trig}} < 1.5$ GeV/c and $3 < p_{\mathrm{T}}^{\mathrm{trig}} < 3.5$ GeV/c, with $p_{\mathrm{T}}^{\mathrm{assoc}}$ fixed at 1–1.5 GeV/c, are presented in Fig. 5 for various centrality ranges. The values of $V_{n\Delta}$ peak at $n = 2$ and then drop dramatically toward larger n values at all centralities, although this behaviour is less pronounced for the 0–5 % centrality bin. The error bars show the statistical uncertainties only, while the systematic uncertainties are indicated in Table 2.

5.1 Factorisation of Fourier coefficients

If the observed azimuthal dihadron correlations at large $\Delta\eta$ are driven only by the single-particle azimuthal anisotropy with respect to a particular direction in the event, the extracted Fourier coefficients ($V_{n\Delta}$) from long-range azimuthal dihadron correlations can be factorised into a product of the single-particle azimuthal anisotropy harmonics, v_n, via

$$V_{n\Delta}\left(p_{\mathrm{T}}^{\mathrm{trig}}, p_{\mathrm{T}}^{\mathrm{assoc}}\right) = v_n\left(p_{\mathrm{T}}^{\mathrm{trig}}\right) \times v_n\left(p_{\mathrm{T}}^{\mathrm{assoc}}\right), \tag{7}$$

Table 2 Systematic uncertainties of the Fourier coefficients ($V_{n\Delta}$) for the first five terms

Source	Systematic uncertainty of $V_{n\Delta}$ (%)
Tracking efficiency	0.8
Vertex dependence	0.5
Track selection dependence	0.5
Finite bin width in $\Delta\phi$	0.3–2.2
Number of terms included in the fit	0.0–1.0
Total	1.1–2.6

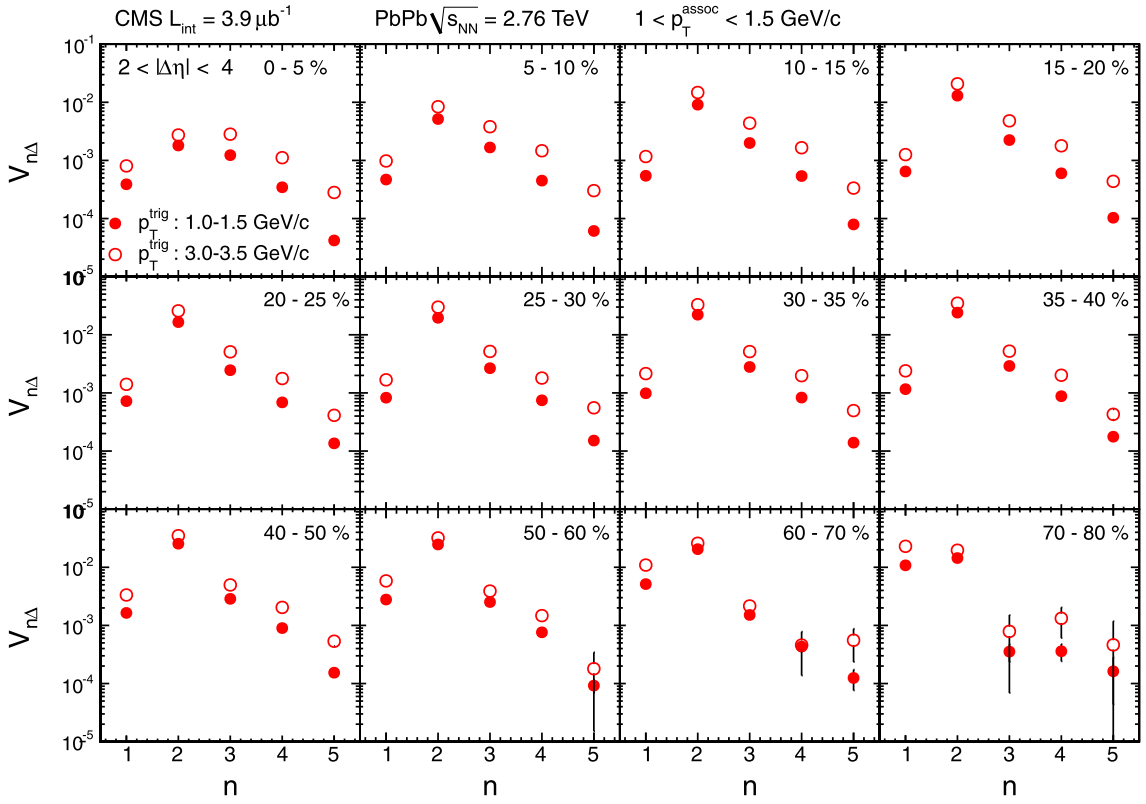

Fig. 5 Fourier coefficients $V_{1\Delta}$ through $V_{5\Delta}$, extracted from the long-range ($2 < |\Delta\eta| < 4$) azimuthal dihadron correlations, for $1 < p_{\mathrm{T}}^{\mathrm{trig}} < 1.5$ GeV/c (*closed circles*) and $3 < p_{\mathrm{T}}^{\mathrm{trig}} < 3.5$ GeV/c (*open circles*) with $p_{\mathrm{T}}^{\mathrm{assoc}}$ fixed at 1–1.5 GeV/c, for twelve centrality intervals. Most of the statistical *error bars* are smaller than the marker size. The systematic uncertainties (not shown in the plots) are indicated in Table 2

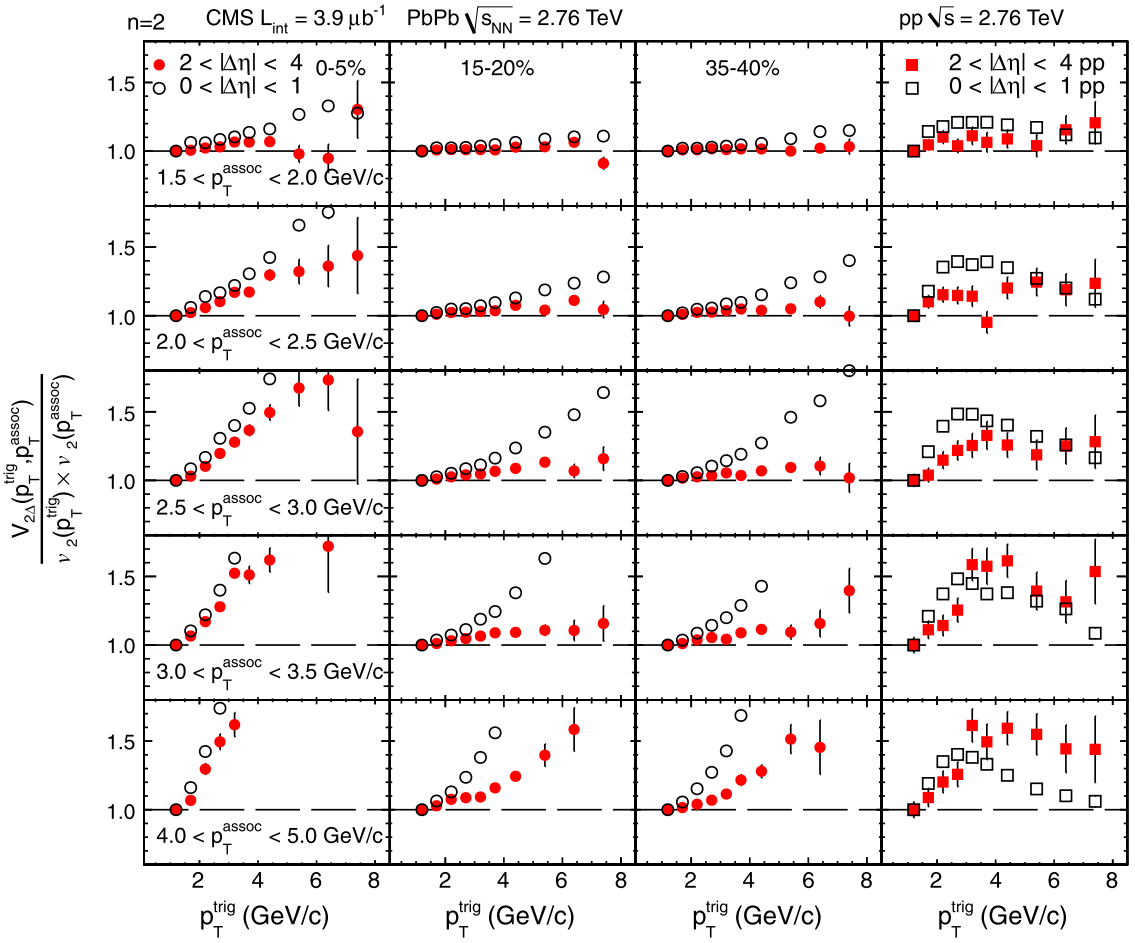

Fig. 6 The ratios of $V_{2\Delta}(p_{\mathrm{T}}^{\mathrm{trig}}, p_{\mathrm{T}}^{\mathrm{assoc}})$ to the product of $v_2(p_{\mathrm{T}}^{\mathrm{trig}})$ and $v_2(p_{\mathrm{T}}^{\mathrm{assoc}})$ for $n = 2$ in the short-range ($0 < |\Delta\eta| < 1$, *open circles*) and long-range ($2 < |\Delta\eta| < 4$, *closed circles*) regions, where $v_2(p_{\mathrm{T}})$ is evaluated in a fixed $p_{\mathrm{T}}^{\mathrm{low}}$ bin of 1–1.5 GeV/c, for five intervals of $p_{\mathrm{T}}^{\mathrm{assoc}}$ and centralities of 0–5 %, 15–20 % and 35–40 %. The *error bars* correspond to statistical uncertainties only

where $v_n(p_{\mathrm{T}}^{\mathrm{trig}})$ and $v_n(p_{\mathrm{T}}^{\mathrm{assoc}})$ are the harmonics for the trigger and associated particles [2] averaged over all the events, respectively. One source of v_n is the collective-flow harmonics arising from hydrodynamic expansion of the medium (e.g., anisotropic elliptic flow contribution to v_2) [42], particularly in the low-p_{T} regime where hadron production in heavy ion collisions is thought to be mainly from the bulk medium [43]. In addition, for very high p_{T} particles that are predominantly produced by the fragmentation of energetic jets, v_n could also be induced by the path-length dependence of the jet-quenching effect inside the medium [44–49]. This path difference can lead to a stronger suppression of the high-p_{T} hadron yield along the long axis of the elliptically-shaped system than along its short axis, resulting in an azimuthal anisotropy characterised by the v_2 harmonic. Both scenarios satisfy the factorisation relation of Eq. (7). However, note that the p_{T} dependent event-by-event fluctuations of v_n could break the factorisation in general, even though v_n may be still related to the single-particle azimuthal anisotropy. This possibility is not investigated in this paper.

This relation (Eq. (7)) is a necessary ingredient for the extraction of single-particle azimuthal anisotropy harmonics using the dihadron correlation data, since a Fourier series can be used to decompose any functional form by construction. The relation can be tested by first assuming that factorisation is valid for pairs including one particle in a fixed, low $p_{\mathrm{T}}^{\mathrm{assoc}}$ range, denoted by $p_{\mathrm{T}}^{\mathrm{low}}$, correlated with a second particle of any p_{T}. The range of $p_{\mathrm{T}}^{\mathrm{low}}$ is chosen to be 1–1.5 GeV/c, where particle production is expected to be predominantly driven by hydrodynamics. The value of $v_n(p_{\mathrm{T}}^{\mathrm{low}})$ is first calculated as the square root of $V_{n\Delta}(p_{\mathrm{T}}^{\mathrm{low}}, p_{\mathrm{T}}^{\mathrm{low}})$. The $v_n(p_{\mathrm{T}}^{\mathrm{trig}})$ is then derived as

$$v_n\left(p_{\mathrm{T}}^{\mathrm{trig}}\right) = \frac{V_{n\Delta}(p_{\mathrm{T}}^{\mathrm{trig}}, p_{\mathrm{T}}^{\mathrm{low}})}{v_n(p_{\mathrm{T}}^{\mathrm{low}})}. \tag{8}$$

This is effectively equivalent to the two-particle cumulant method of flow measurement [50, 51]. Next, the ratio of

$V_{n\Delta}(p_{\mathrm{T}}^{\mathrm{trig}}, p_{\mathrm{T}}^{\mathrm{assoc}})$ directly extracted as a function of $p_{\mathrm{T}}^{\mathrm{trig}}$ and $p_{\mathrm{T}}^{\mathrm{assoc}}$ (left-hand side of Eq. (7)) to the product of $v_n(p_{\mathrm{T}}^{\mathrm{trig}})$ and $v_n(p_{\mathrm{T}}^{\mathrm{assoc}})$ (right-hand side of Eq. (7)) is calculated. This ratio should be approximately unity if factorisation is also valid for higher $p_{\mathrm{T}}^{\mathrm{trig}}$ and $p_{\mathrm{T}}^{\mathrm{assoc}}$ particles.

Figures 6, 7, and 8 show the ratios for $n = 2$, 3, and 4, over five $p_{\mathrm{T}}^{\mathrm{assoc}}$ ranges as a function of $p_{\mathrm{T}}^{\mathrm{trig}}$, for both short-range ($0 < |\Delta\eta| < 1$) and long-range ($2 < |\Delta\eta| < 4$) regions. Three different centrality intervals 0–5 %, 15–20 % and 35–40 % are presented. The ratio for $n = 2$ in pp data is also shown in the last column of Fig. 6. The first point of each panel equals 1.0 by construction. The error bars correspond to the statistical uncertainties. The total systematic uncertainties are estimated to be 1.5 % ($n = 2$)–3.6 % ($n = 5$), approximately $\sqrt{2}$ times the systematic uncertainties of $V_{n\Delta}$ shown in Table 2.

First of all, no evidence of factorisation is found in the pp data and for the short-range region ($0 < |\Delta\eta| < 1$) in any of the centrality ranges of the PbPb data, where dijet production is expected to be the dominant source of correlations. In Ref. [2], it has been shown that $V_{n\Delta}$ factorises for jet-like correlations at very high-p_{T} (e.g., $p_{\mathrm{T}} > 5$ GeV/c) forms a special axis, to which produced particles are strongly correlated. This is similar to the elliptic flow effect, where particles are preferentially produced along the short axis of the elliptically-shaped overlapping region. However, the lack of factorisation in pp and the short-range region of PbPb observed for the p_{T} range of $1 < p_{\mathrm{T}}^{\mathrm{assoc}} < 3.5$ GeV/c primarily investigated in this paper may suggest a complicated interplay of different particle production mechanisms between low-p_{T} (hydrodynamic flow for PbPb and underlying event for pp) and high-p_{T} (dijet production) particles.

In contrast, the long-range region ($2 < |\Delta\eta| < 4$) for mid-peripheral 15–20 % and 35–40 % events does show evidence of factorisation for $V_{2\Delta}$ to $V_{4\Delta}$ with $p_{\mathrm{T}}^{\mathrm{assoc}}$ up to 3–3.5 GeV/c and $p_{\mathrm{T}}^{\mathrm{trig}}$ up to approximately 8 GeV/c. The data are also consistent with factorisation for even higher $p_{\mathrm{T}}^{\mathrm{trig}}$ (> 8 GeV/c) combined with low $p_{\mathrm{T}}^{\mathrm{assoc}}$, but the current event sample is not large enough to draw a firm conclusion. Note that $V_{n\Delta}$ varies by almost 60 % in the $p_{\mathrm{T}}^{\mathrm{trig}}$ range from 1 to 3.5 GeV/c as shown in Fig. 5, whereas factorisation is found to hold to better than 5 %. This suggests a potential connection between the extracted Fourier coefficients from long-range dihadron correlations and the single-particle azimuthal anisotropy harmonics. For the most central 0–5 % collisions, the ratio for $n = 2$ deviates significantly from unity, while $V_{3\Delta}$ and $V_{4\Delta}$ still show a similar level of factorisation to that of the 15–20 % and 35–40 %

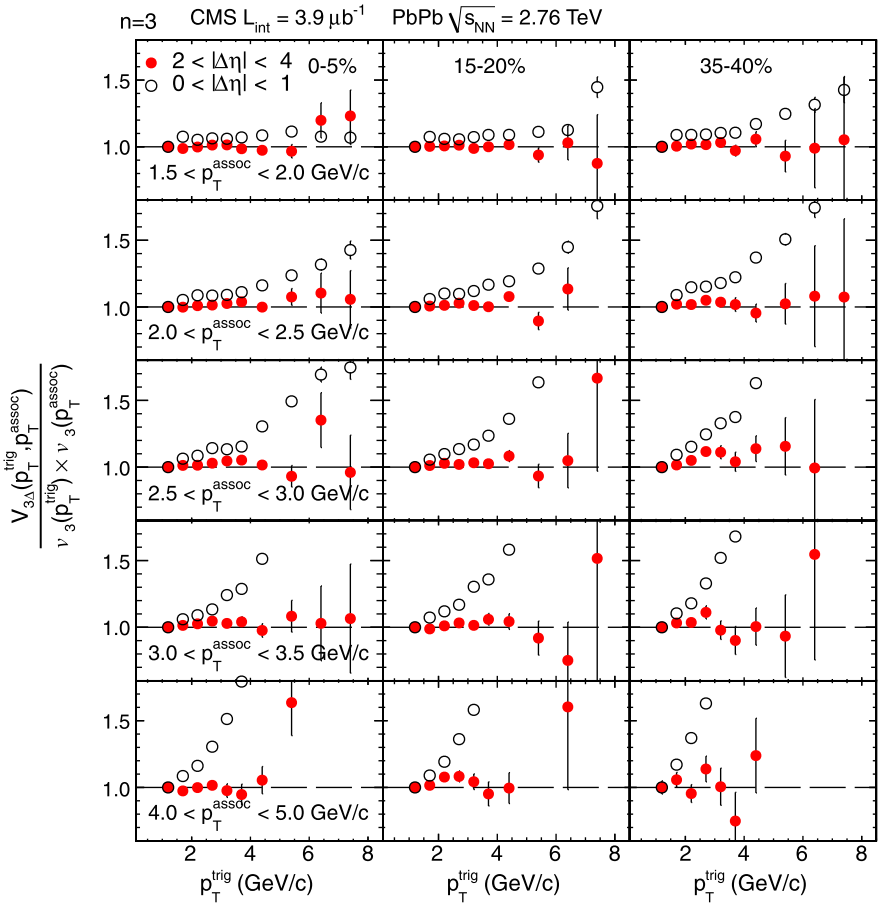

Fig. 7 The ratios of $V_{3\Delta}(p_{\mathrm{T}}^{\mathrm{trig}}, p_{\mathrm{T}}^{\mathrm{assoc}})$ to the product of $v_3(p_{\mathrm{T}}^{\mathrm{trig}})$ and $v_3(p_{\mathrm{T}}^{\mathrm{assoc}})$ for $n = 3$ in the short-range ($0 < |\Delta\eta| < 1$, *open circles*) and long-range ($2 < |\Delta\eta| < 4$, *closed circles*) regions, where $v_3(p_{\mathrm{T}})$ is evaluated in a fixed $p_{\mathrm{T}}^{\mathrm{low}}$ bin of 1–1.5 GeV/c, for five intervals of $p_{\mathrm{T}}^{\mathrm{assoc}}$ and centralities of 0–5 %, 15–20 % and 35–40 %. The error bars correspond to statistical uncertainties only

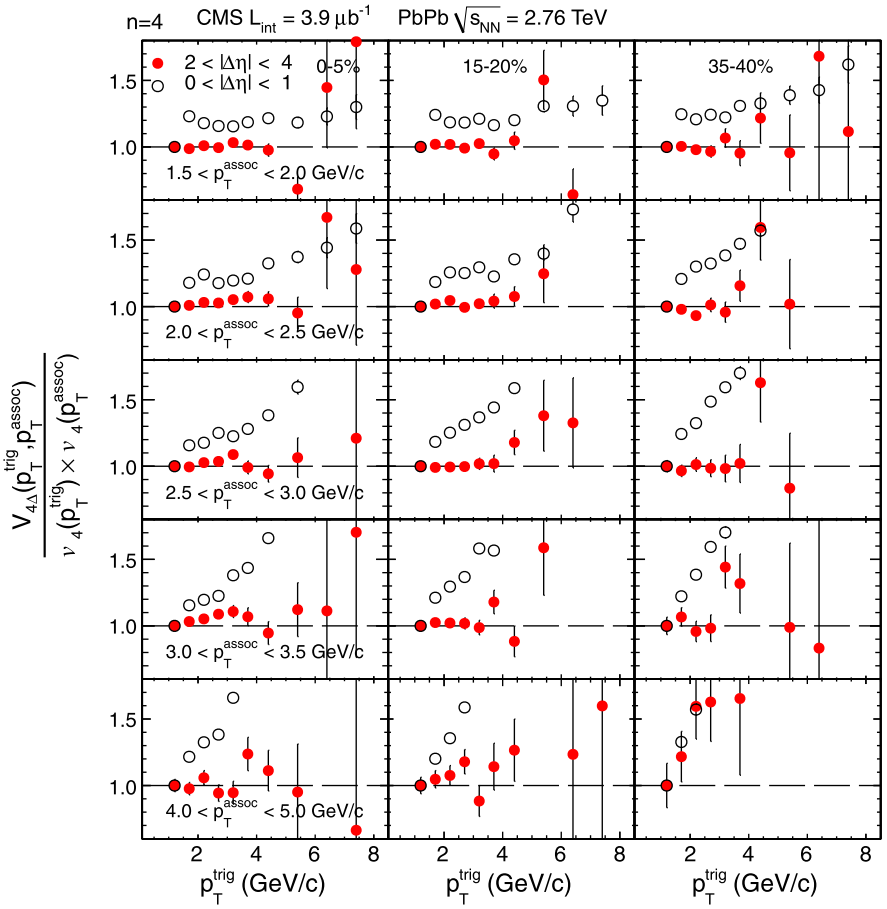

Fig. 8 The ratios of $V_{4\Delta}(p_{\mathrm{T}}^{\mathrm{trig}}, p_{\mathrm{T}}^{\mathrm{assoc}})$ to the product of $v_4(p_{\mathrm{T}}^{\mathrm{trig}})$ and $v_4(p_{\mathrm{T}}^{\mathrm{assoc}})$ for $n = 4$ in the short-range ($0 < |\Delta\eta| < 1$, *open circles*) and long-range ($2 < |\Delta\eta| < 4$, *closed circles*) regions, where $v_4(p_{\mathrm{T}})$ is evaluated in a fixed $p_{\mathrm{T}}^{\mathrm{low}}$ bin of 1–1.5 GeV/c, for five intervals of $p_{\mathrm{T}}^{\mathrm{assoc}}$ and centralities of 0–5 %, 15–20 % and 35–40 %. The *error bars* correspond to statistical uncertainties only

mid-peripheral data. This may indicate the existence of other sources of long-range correlations for the most central collisions that violate the factorisation relation. The breakdown of factorisation for $p_{\mathrm{T}}^{\mathrm{assoc}} > 4$ GeV/c in the long-range region is likely due to dijet correlations. Higher-order Fourier coefficients and a wider p_{T} range can be investigated once larger samples of PbPb data are collected. Factorisation of $V_{1\Delta}$ is not discussed in this paper as it contains an additional negative contribution from momentum conservation [52], which is not related to the collective flow effect and needs to be accounted for in further studies.

5.2 Elliptic and higher-order single-particle azimuthal anisotropy harmonics

As discussed in Sect. 5.1, except for v_2 in the very central PbPb events, the factorisation relation given by Eq. (7) for long-range ($2 < |\Delta\eta| < 4$) azimuthal dihadron correlations is found to be valid for sufficiently low $p_{\mathrm{T}}^{\mathrm{assoc}}$, combined with low $p_{\mathrm{T}}^{\mathrm{trig}}$, and possibly high $p_{\mathrm{T}}^{\mathrm{trig}}$ as well. Therefore, the single-particle azimuthal anisotropy harmonics $v_n(p_{\mathrm{T}}^{\mathrm{trig}})$ can be extracted using Eq. (8) with $1 < p_{\mathrm{T}}^{\mathrm{assoc}} < 3$ GeV/c. Values are found for centralities ranging from 0–5 % to 70–80 %, and presented in Fig. 9. The 1–3 GeV/c $p_{\mathrm{T}}^{\mathrm{assoc}}$ range is chosen in order to reduce the statistical uncertainty by utilising as many associated particles as possible over the $p_{\mathrm{T}}^{\mathrm{assoc}}$ range where factorisation is valid. Data for the most central and most peripheral events are included for completeness, although the results for v_2 in those events are clearly demonstrated by Fig. 6 to be more complicated in nature. The value of v_2 is extracted up to $p_{\mathrm{T}}^{\mathrm{trig}} \sim 20$ GeV/c for all but the 2 most peripheral centralities, whereas higher-order v_n are truncated at $p_{\mathrm{T}}^{\mathrm{trig}} \sim 10$ GeV/c or less for the peripheral data due to statistical limitations. As mentioned previously, factorisation is not demonstrated conclusively at very high $p_{\mathrm{T}}^{\mathrm{trig}}$. For the most central 0–5 % events, all the harmonics are of similar magnitude across the entire $p_{\mathrm{T}}^{\mathrm{trig}}$ range. The p_{T} dependence of all v_n shows the same trend of a fast rise to a maximum around $p_{\mathrm{T}} \approx 3$ GeV/c, followed by a slower fall, independent of centrality up to 50–60 %. The magnitude of v_2 increases when moving away from the most central events. At very high $p_{\mathrm{T}}^{\mathrm{trig}}$, sizeable v_2 signals are observed, which exhibit an almost flat p_{T} dependence from 10 to 20 GeV/c for most of the centrality ranges. This is not the case for the higher-order harmonics. In order to explicitly investigate the centrality dependence of the harmonics, the extracted v_2 through v_5 are also shown in Fig. 10 as

a function of N_{part}, for representative low (1–1.5 GeV/c), intermediate (3–3.5 GeV/c), and high (8–20 GeV/c) $p_{\text{T}}^{\text{trig}}$ ranges.

A strong centrality dependence of v_2 is observed in Figs. 9 and 10 for all $p_{\text{T}}^{\text{trig}}$ ranges, while the higher-order harmonics v_3–v_5 do not vary significantly over the range of N_{part}. This behaviour is expected in the context of both the hydrodynamic flow phenomena for lower-p_{T} particles [43] and the path-length dependence of the parton energy-loss scenario for high-p_{T} particles [44]. The v_2 harmonics are sensitive to the eccentricity of the almond-shaped initial collision region that becomes larger for the peripheral events, whereas the higher-order harmonics are driven by fluctuations of the initial geometry that have little dependence on

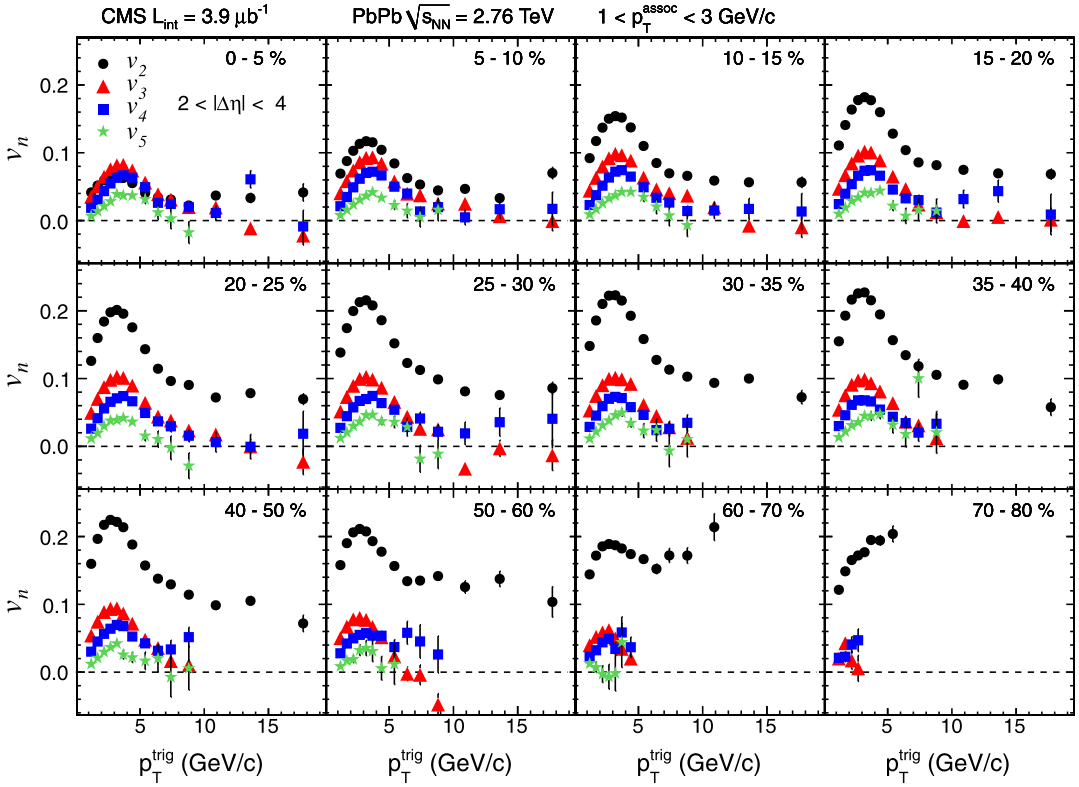

Fig. 9 The single-particle azimuthal anisotropy harmonics v_2–v_5 extracted from the long-range ($2 < |\Delta\eta| < 4$) azimuthal dihadron correlations as a function of $p_{\text{T}}^{\text{trig}}$, combined with $1 < p_{\text{T}}^{\text{assoc}} < 3$ GeV/c, for twelve centrality intervals in PbPb collisions at $\sqrt{s_{NN}} = 2.76$ TeV. Most of the statistical *error bars* are smaller than the marker size. The systematic uncertainties (not shown in the plots) are indicated in Table 2

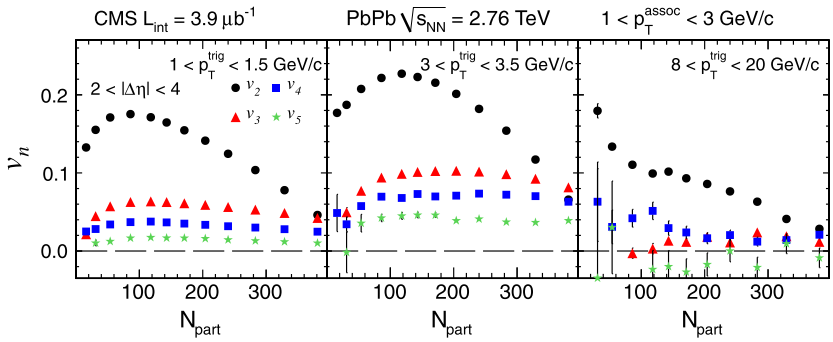

Fig. 10 The single-particle azimuthal anisotropy harmonics, v_2–v_5, extracted from the long-range ($2 < |\Delta\eta| < 4$) azimuthal dihadron correlations as a function of N_{part} in PbPb collisions at $\sqrt{s_{NN}} = 2.76$ TeV for $1 < p_{\text{T}}^{\text{assoc}} < 3$ GeV/c in three $p_{\text{T}}^{\text{trig}}$ ranges of 1–1.5, 3–3.5 and 8–20 GeV/c. Most of the statistical *error bars* are smaller than the marker size. The systematic uncertainties (not shown in the plots) are indicated in Table 2

the collision centrality [53]. In the most peripheral events, the p_{T} dependence of v_2 is found to be very different from that in the central events, as shown in Fig. 9. In the high-p_{T} interval 8–20 GeV/c (third panel of Fig. 10), v_2 increases rapidly at low N_{part} (very peripheral). A possible explanation is the presence of non-flow effects due to back-to-back jets. Based on the factorised Fourier coefficients from long-range dihadron correlations, the single-particle azimuthal anisotropy harmonics extracted over a wide range of p_{T} and centrality allow a detailed comparison to theoretical calculations of the hydrodynamics and path-length dependence of in-medium parton energy loss.

6 Summary

The previous CMS analysis of angular correlations between charged particles has been expanded to cover a wide centrality range of PbPb collisions at $\sqrt{s_{NN}} = 2.76$ TeV. As was seen previously for central PbPb collisions, the associated yields differ significantly from those observed in pp interactions. Correlations with both small ($0 < |\Delta\eta| < 1$) and large ($2 < |\Delta\eta| < 4$) relative pseudorapidities were again studied as a function of the transverse momentum of the trigger and associated particle p_{T}. The integrated yield of the near-side region shows an increasing enhancement towards more central PbPb collisions, especially for low-p_{T} associated particles.

To further characterise the dependence of the correlations on relative azimuthal angle, a Fourier decomposition of the distributions projected onto $\Delta\phi$ was performed, as a function of both centrality and particle p_{T}. Evidence of a factorisation relation was observed between the Fourier coefficients ($V_{n\Delta}$) from dihadron correlations and single-particle azimuthal anisotropy harmonics (v_n). This holds for $p_{\mathrm{T}}^{\mathrm{assoc}} \lesssim 3$–$3.5$ GeV/c over the $p_{\mathrm{T}}^{\mathrm{trig}}$ range up to at least 8 GeV/c in central and mid-peripheral PbPb collisions, except for v_2 in the most central events. The observed factorisation is absent in pp and very peripheral PbPb data, indicating a strong connection of the observed long-range azimuthal dihadron correlations to the single-particle azimuthal anisotropy in heavy ion collisions, such as the one driven by the hydrodynamic expansion of the system. The single-particle azimuthal anisotropy harmonics v_2 through v_5 were extracted over a wide range in both p_{T} and collision centrality, profiting from the broad solid-angle coverage of the CMS detector. The comprehensive correlation data presented in this paper are very useful for studies of the path-length dependence of in-medium parton energy-loss, and provide valuable inputs to a variety of theoretical models, including hydrodynamic calculations of higher-order Fourier components.

Acknowledgements We wish to congratulate our colleagues in the CERN accelerator departments for the excellent performance of the LHC machine. We thank the technical and administrative staff at CERN and other CMS institutes, and acknowledge support from: FMSR (Austria); FNRS and FWO (Belgium); CNPq, CAPES, FAPERJ, and FAPESP (Brazil); MES (Bulgaria); CERN; CAS, MoST, and NSFC (China); COLCIENCIAS (Colombia); MSES (Croatia); RPF (Cyprus); Academy of Sciences and NICPB (Estonia); Academy of Finland, MEC, and HIP (Finland); CEA and CNRS/IN2P3 (France); BMBF, DFG, and HGF (Germany); GSRT (Greece); OTKA and NKTH (Hungary); DAE and DST (India); IPM (Iran); SFI (Ireland); INFN (Italy); NRF and WCU (Korea); LAS (Lithuania); CINVESTAV, CONACYT, SEP, and UASLP-FAI (Mexico); MSI (New Zealand); PAEC (Pakistan); SCSR (Poland); FCT (Portugal); JINR (Armenia, Belarus, Georgia, Ukraine, Uzbekistan); MON, RosAtom, RAS and RFBR (Russia); MSTD (Serbia); MICINN and CPAN (Spain); Swiss Funding Agencies (Switzerland); NSC (Taipei); TUBITAK and TAEK (Turkey); STFC (United Kingdom); DOE and NSF (USA).

Individuals have received support from the Marie-Curie programme and the European Research Council (European Union); the Leventis Foundation; the A.P. Sloan Foundation; the Alexander von Humboldt Foundation; the Belgian Federal Science Policy Office; the Fonds pour la Formation à la Recherche dans l'Industrie et dans l'Agriculture (FRIA-Belgium); the Agentschap voor Innovatie door Wetenschap en Technologie (IWT-Belgium); and the Council of Science and Industrial Research, India.

References

1. CMS Collaboration, Long-range and short-range dihadron angular correlations in central Pb Pb collisions at $\sqrt{s_{NN}} =$ 2.76 TeV. J. High Energy Phys. **07**, 076 (2011). doi:10.1007/JHEP07(2011)076, arXiv:1105.2438
2. ALICE Collaboration, Harmonic decomposition of two-particle angular correlations in Pb–Pb collisions at $\sqrt{s_{NN}} = 2.76$ TeV (2011). arXiv:1109.2501
3. STAR Collaboration, Disappearance of back-to-back high p_T hadron correlations in central Au + Au collisions at $\sqrt{s_{NN}} =$ 200 GeV. Phys. Rev. Lett. **90**, 082302 (2003). doi:10.1103/PhysRevLett.90.082302, arXiv:nucl-ex/0210033
4. STAR Collaboration, Long range rapidity correlations and jet production in high energy nuclear collisions. Phys. Rev. C **80**, 064912 (2009). doi:10.1103/PhysRevC.80.064912, arXiv:0909.0191
5. STAR Collaboration, System size dependence of associated yields in hadron-triggered jets. Phys. Lett. B **683**, 123 (2010). doi:10.1103/PhysRevC.80.064912, arXiv:0909.0191
6. STAR Collaboration, Distributions of charged hadrons associated with high transverse momentum particles in pp and Au+Au collisions at $\sqrt{s_{NN}} = 200$ GeV. Phys. Rev. Lett. **95**, 152301 (2005). doi:10.1103/PhysRevLett.95.152301, arXiv:nucl-ex/0501016
7. PHENIX Collaboration, System size and energy dependence of jet-induced hadron pair correlation shapes in Cu+Cu and Au+Au collisions at $\sqrt{s_{NN}} = 200$ and 62.4 GeV. Phys. Rev. Lett. **98**, 232302 (2007). doi:10.1103/PhysRevLett.98.232302, arXiv:nucl-ex/0611019
8. PHENIX Collaboration, Dihadron azimuthal correlations in Au + Au collisions at $\sqrt{s_{NN}} = 200$ GeV. Phys. Rev. C **78**, 014901 (2008). doi:10.1103/PhysRevC.78.014901, arXiv:0801.4545

9. PHOBOS Collaboration, High transverse momentum triggered correlations over a large pseudorapidity acceptance in Au + Au collisions at $\sqrt{s_{NN}} = 200$ GeV. Phys. Rev. Lett. **104**, 062301 (2010). doi:10.1103/PhysRevLett.104.062301, arXiv:0903.2811
10. PHOBOS Collaboration, System size dependence of cluster properties from two-particle angular correlations in Cu + Cu and Au + Au collisions at $\sqrt{s_{NN}} = 200$ GeV. Phys. Rev. C **81**, 024904 (2010). doi:10.1103/PhysRevC.81.024904, arXiv:0812.1172
11. ALICE Collaboration, Suppression of charged particle production at large transverse momentum in central Pb–Pb collisions at $\sqrt{s_{NN}} = 2.76$ TeV. Phys. Lett. B **696**, 30 (2011). doi:10.1016/j.physletb.2010.12.020, arXiv:1012.1004
12. ATLAS Collaboration, Observation of a centrality-dependent dijet asymmetry in lead–lead collisions at $\sqrt{s_{NN}} = 2.76$ TeV with the ATLAS detector at the LHC. Phys. Rev. Lett. **105**, 252303 (2010). doi:10.1103/PhysRevLett.105.252303, arXiv:1011.6182
13. CMS Collaboration, Observation and studies of jet quenching in PbPb collisions at nucleon–nucleon center-of-mass energy = 2.76 TeV. Phys. Rev. C **84**, 024906 (2011). doi:10.1103/PhysRevC.84.024906, arXiv:1102.1957
14. N. Armesto, C.A. Salgado, U.A. Wiedemann, Measuring the collective flow with jets. Phys. Rev. Lett. **93**, 242301 (2004). doi:10.1103/PhysRevLett.93.242301, arXiv:hep-ph/0405301
15. A. Majumder, B. Muller, S.A. Bass, Longitudinal broadening of quenched jets in turbulent color fields. Phys. Rev. Lett. **99**, 042301 (2007). doi:10.1103/PhysRevLett.99.042301, arXiv:hep-ph/0611135
16. C.B. Chiu, R.C. Hwa, Pedestal and peak structure in jet correlation. Phys. Rev. C **72**, 034903 (2005). doi:10.1103/PhysRevC.72.034903, arXiv:nucl-th/0505014
17. C.-Y. Wong, Momentum kick model description of the near-side ridge and jet quenching. Phys. Rev. C **78**, 064905 (2008). doi:10.1103/PhysRevC.78.064905, arXiv:0806.2154
18. P. Romatschke, Momentum broadening in an anisotropic plasma. Phys. Rev. C **75**, 014901 (2007). doi:10.1103/PhysRevC.75.014901, arXiv:hep-ph/0607327
19. E.V. Shuryak, On the origin of the "ridge" phenomenon induced by jets in heavy ion collisions. Phys. Rev. C **76**, 047901 (2007). doi:10.1103/PhysRevC.76.047901, arXiv:0706.3531
20. S.A. Voloshin, Two particle rapidity, transverse momentum, and azimuthal correlations in relativistic nuclear collisions and transverse radial expansion. Nucl. Phys. A **749**, 287 (2005). doi:10.1016/j.nuclphysa.2004.12.053, arXiv:nucl-th/0410024
21. A.P. Mishra et al., Super-horizon fluctuations and acoustic oscillations in relativistic heavy-ion collisions. Phys. Rev. C **77**, 064902 (2008). doi:10.1103/PhysRevC.77.064902, arXiv:0711.1323
22. J. Takahashi et al., Topology studies of hydrodynamics using two particle correlation analysis. Phys. Rev. Lett. **103**, 242301 (2009). doi:10.1103/PhysRevLett.103.242301, arXiv:0902.4870
23. B. Alver, G. Roland, Collision-geometry fluctuations and triangular flow in heavy-ion collisions. Phys. Rev. C **81**, 054905 (2010). doi:10.1103/PhysRevC.81.054905, arXiv:1003.0194
24. B.H. Alver et al., Triangular flow in hydrodynamics and transport theory. Phys. Rev. C **82**, 034913 (2010). doi:10.1103/PhysRevC.82.034913, arXiv:1007.5469
25. B. Schenke, S. Jeon, C. Gale, Elliptic and triangular flow in event-by-event $D = (3 + 1)$ viscous hydrodynamics. Phys. Rev. Lett. **106**, 042301 (2011). doi:10.1103/PhysRevLett.106.042301, arXiv:1009.3244
26. H. Petersen et al., Triangular flow in event-by-event ideal hydrodynamics in Au+Au collisions at $\sqrt{s_{NN}} = 200$ GeV. Phys. Rev. C **82**, 041901 (2010). doi:10.1103/PhysRevC.82.041901, arXiv:1008.0625
27. J. Xu, C.M. Ko, Effects of triangular flow on di-hadron azimuthal correlations in relativistic heavy ion collisions. Phys. Rev. C **83**, 021903 (2011). doi:10.1103/PhysRevC.83.021903, arXiv:1011.3750
28. D. Teaney, L. Yan, Triangularity and dipole asymmetry in heavy ion collisions. Phys. Rev. C **83**, 064904 (2011). doi:10.1103/PhysRevC.83.064904, arXiv:1010.1876
29. ALICE Collaboration, Higher harmonic anisotropic flow measurements of charged particles in Pb–Pb collisions at $\sqrt{s_{NN}} = 2.76$ TeV. Phys. Rev. Lett. **107**, 032301 (2011). arXiv:1105.3865
30. CMS Collaboration, Observation of long-range near-side angular correlations in proton–proton collisions at the LHC. J. High Energy Phys. **09**, 091 (2010). doi:10.1007/JHEP09(2010)091, arXiv:1009.4122
31. CMS Collaboration, The CMS experiment at the CERN LHC. J. Instrum. **0803**, S08004 (2008). doi:10.1088/1748-0221/3/08/S08004
32. CMS Collaboration, Measurement of CMS luminosity. CMS Physics Analysis Summary CMS-PAS-EWK-10-004 (2010)
33. CMS Collaboration, Absolute luminosity normalization. CMS Detector Performance Summary CMS-DP-2011-002 (2011)
34. M.L. Miller et al., Glauber modeling in high-energy nuclear collisions. Annu. Rev. Nucl. Part. Sci. **57**, 205 (2007). doi:10.1146/annurev.nucl.57.090506.123020
35. B. Alver et al., The PHOBOS Glauber Monte Carlo (2008). arXiv:0805.4411
36. CMS Collaboration, Dependence on pseudorapidity and centrality of charged hadron production in PbPb collisions at a nucleon–nucleon centre-of-mass energy of 2.76 TeV. J. High Energy Phys. **08**, 141 (2011). doi:10.1007/JHEP08(2011)141, arXiv:1107.4800
37. CMS Collaboration, CMS physics technical design report: Addendum on high density QCD with heavy ions. J. Phys. G **34**, 2307 (2007). doi:10.1088/0954-3899/34/11/008
38. CMS Collaboration, Tracking and vertexing results from first collisions. CMS Physics Analysis Summary CMS-PAS-TRK-10-001 (2010)
39. I.P. Lokhtin, A.M. Snigirev, A model of jet quenching in ultrarelativistic heavy ion collisions and high-p_{T} hadron spectra at RHIC. Eur. Phys. J. C **45**, 211 (2006). doi:10.1140/epjc/s2005-02426-3, arXiv:hep-ph/0506189
40. J. Putschke, Intra-jet correlations of high-p_t hadrons from STAR. J. Phys. G **34**, S679 (2007). doi:10.1088/0954-3899/34/8/S72, arXiv:nucl-ex/0701074
41. STAR Collaboration, Anomalous centrality evolution of two-particle angular correlations from Au–Au collisions at $\sqrt{s_{NN}} =$ 62 and 200 GeV. arXiv:1109.4380
42. S. Voloshin, Y. Zhang, Flow study in relativistic nuclear collisions by Fourier expansion of azimuthal particle distributions. Z. Phys. C **70**, 665 (1996). doi:10.1007/s002880050141, arXiv:hep-ph/9407282
43. S.A. Voloshin, A.M. Poskanzer, R. Snellings, Collective phenomena in non-central nuclear collisions. arXiv:0809.2949
44. PHENIX Collaboration, Azimuthal anisotropy of neutral pion production in Au + Au collisions at $\sqrt{s_{NN}} = 200$ GeV: Path-length dependence of jet quenching and the role of initial geometry. Phys. Rev. Lett. **105**, 142301 (2010). doi:10.1103/PhysRevLett.105.142301, arXiv:1006.3740
45. S.A. Bass et al., Systematic comparison of jet energy-loss schemes in a realistic hydrodynamic medium. Phys. Rev. C **79**, 024901 (2009). doi:10.1103/PhysRevC.79.024901, arXiv:0808.0908
46. S. Peigné, A.V. Smilga, Energy losses in a hot plasma revisited: QCD versus QED. Phys. Usp. **52**, 659 (2009). doi:10.3367/UFNe.0179.200907a.0697, arXiv:0810.5702. Usp. Fiz. Nauk **179**, 697 (2009)
47. S.S. Gubser et al., Gluon energy loss in the gauge–string duality. J. High Energy Phys. **10**, 052 (2008). doi:10.1088/1126-6708/2008/10/052, arXiv:0803.1470
48. S. Wicks et al., Elastic, inelastic, and path length fluctuations in jet tomography. Nucl. Phys. A **784**, 426 (2007). doi:10.1016/j.nuclphysa.2006.12.048, arXiv:nucl-th/0512076

49. C. Marquet, T. Renk, Jet quenching in the strongly-interacting quark–gluon plasma. Phys. Lett. B **685**, 270 (2010). doi:10.1016/j.physletb.2010.01.076, arXiv:0908.0880
50. N. Borghini et al., A New method for measuring azimuthal distributions in nucleus–nucleus collisions. Phys. Rev. C **63**, 054906 (2001). doi:10.1103/PhysRevC.63.054906, arXiv:nucl-th/0007063
51. N. Borghini et al., Flow analysis from multiparticle azimuthal correlations. Phys. Rev. C **64**, 054901 (2001). doi:10.1103/PhysRevC.64.054901, arXiv:nucl-th/0105040
52. M. Luzum, J.-Y. Ollitrault, Directed flow at midrapidity in heavy-ion collisions. Phys. Rev. Lett. **106**, 102301 (2011). doi:10.1103/PhysRevLett.106.102301, arXiv:1011.6361
53. B. Alver et al., Importance of correlations and fluctuations on the initial source eccentricity in high-energy nucleus–nucleus collisions. Phys. Rev. C **77**, 014906 (2008). doi:10.1103/PhysRevC.77.014906, arXiv:0711.3724

The CMS Collaboration

Yerevan Physics Institute, Yerevan, Armenia
S. Chatrchyan, V. Khachatryan, A.M. Sirunyan, A. Tumasyan

Institut für Hochenergiephysik der OeAW, Wien, Austria
W. Adam, T. Bergauer, M. Dragicevic, J. Erö, C. Fabjan, M. Friedl, R. Frühwirth, V.M. Ghete, J. Hammer[1], M. Hoch, N. Hörmann, J. Hrubec, M. Jeitler, W. Kiesenhofer, A. Knapitsch, M. Krammer, D. Liko, I. Mikulec, M. Pernicka[†], B. Rahbaran, C. Rohringer, H. Rohringer, R. Schöfbeck, J. Strauss, A. Taurok, F. Teischinger, P. Wagner, W. Waltenberger, G. Walzel, E. Widl, C.-E. Wulz

National Centre for Particle and High Energy Physics, Minsk, Belarus
V. Mossolov, N. Shumeiko, J. Suarez Gonzalez

Universiteit Antwerpen, Antwerpen, Belgium
S. Bansal, L. Benucci, T. Cornelis, E.A. De Wolf, X. Janssen, S. Luyckx, T. Maes, L. Mucibello, S. Ochesanu, B. Roland, R. Rougny, M. Selvaggi, H. Van Haevermaet, P. Van Mechelen, N. Van Remortel, A. Van Spilbeeck

Vrije Universiteit Brussel, Brussel, Belgium
F. Blekman, S. Blyweert, J. D'Hondt, R. Gonzalez Suarez, A. Kalogeropoulos, M. Maes, A. Olbrechts, W. Van Doninck, P. Van Mulders, G.P. Van Onsem, I. Villella

Université Libre de Bruxelles, Bruxelles, Belgium
O. Charaf, B. Clerbaux, G. De Lentdecker, V. Dero, A.P.R. Gay, G.H. Hammad, T. Hreus, A. Léonard, P.E. Marage, L. Thomas, C. Vander Velde, P. Vanlaer, J. Wickens

Ghent University, Ghent, Belgium
V. Adler, K. Beernaert, A. Cimmino, S. Costantini, G. Garcia, M. Grunewald, B. Klein, J. Lellouch, A. Marinov, J. Mccartin, A.A. Ocampo Rios, D. Ryckbosch, N. Strobbe, F. Thyssen, M. Tytgat, L. Vanelderen, P. Verwilligen, S. Walsh, N. Zaganidis

Université Catholique de Louvain, Louvain-la-Neuve, Belgium
S. Basegmez, G. Bruno, J. Caudron, L. Ceard, J. De Favereau De Jeneret, C. Delaere, T. du Pree, D. Favart, L. Forthomme, A. Giammanco[2], G. Grégoire, J. Hollar, V. Lemaitre, J. Liao, O. Militaru, C. Nuttens, D. Pagano, A. Pin, K. Piotrzkowski, N. Schul

Université de Mons, Mons, Belgium
N. Beliy, T. Caebergs, E. Daubie

Centro Brasileiro de Pesquisas Fisicas, Rio de Janeiro, Brazil
G.A. Alves, D. De Jesus Damiao, M.E. Pol, M.H.G. Souza

Universidade do Estado do Rio de Janeiro, Rio de Janeiro, Brazil
W.L. Aldá Júnior, W. Carvalho, A. Custódio, E.M. Da Costa, C. De Oliveira Martins, S. Fonseca De Souza, D. Matos Figueiredo, L. Mundim, H. Nogima, V. Oguri, W.L. Prado Da Silva, A. Santoro, S.M. Silva Do Amaral, L. Soares Jorge, A. Sznajder

Instituto de Fisica Teorica, Universidade Estadual Paulista, Sao Paulo, Brazil
T.S. Anjos[3], C.A. Bernardes[3], F.A. Dias[4], T.R. Fernandez Perez Tomei, E.M. Gregores[3], C. Lagana, F. Marinho, P.G. Mercadante[3], S.F. Novaes, S.S. Padula

Institute for Nuclear Research and Nuclear Energy, Sofia, Bulgaria
V. Genchev[1], P. Iaydjiev[1], S. Piperov, M. Rodozov, S. Stoykova, G. Sultanov, V. Tcholakov, R. Trayanov, M. Vutova

University of Sofia, Sofia, Bulgaria
A. Dimitrov, R. Hadjiiska, A. Karadzhinova, V. Kozhuharov, L. Litov, B. Pavlov, P. Petkov

Institute of High Energy Physics, Beijing, China
J.G. Bian, G.M. Chen, H.S. Chen, C.H. Jiang, D. Liang, S. Liang, X. Meng, J. Tao, J. Wang, J. Wang, X. Wang, Z. Wang, H. Xiao, M. Xu, J. Zang, Z. Zhang

State Key Lab. of Nucl. Phys. and Tech., Peking University, Beijing, China
C. Asawatangtrakuldee, Y. Ban, S. Guo, Y. Guo, W. Li, S. Liu, Y. Mao, S.J. Qian, H. Teng, S. Wang, B. Zhu, W. Zou

Universidad de Los Andes, Bogota, Colombia
A. Cabrera, B. Gomez Moreno, A.F. Osorio Oliveros, J.C. Sanabria

Technical University of Split, Split, Croatia
N. Godinovic, D. Lelas, R. Plestina[5], D. Polic, I. Puljak[1]

University of Split, Split, Croatia
Z. Antunovic, M. Dzelalija, M. Kovac

Institute Rudjer Boskovic, Zagreb, Croatia
V. Brigljevic, S. Duric, K. Kadija, J. Luetic, S. Morovic

University of Cyprus, Nicosia, Cyprus
A. Attikis, M. Galanti, J. Mousa, C. Nicolaou, F. Ptochos, P.A. Razis

Charles University, Prague, Czech Republic
M. Finger, M. Finger Jr.

Academy of Scientific Research and Technology of the Arab Republic of Egypt, Egyptian Network of High Energy Physics, Cairo, Egypt
Y. Assran[6], A. Ellithi Kamel[7], S. Khalil[8], M.A. Mahmoud[9], A. Radi[10]

National Institute of Chemical Physics and Biophysics, Tallinn, Estonia
A. Hektor, M. Kadastik, M. Müntel, M. Raidal, L. Rebane, A. Tiko

Department of Physics, University of Helsinki, Helsinki, Finland
V. Azzolini, P. Eerola, G. Fedi, M. Voutilainen

Helsinki Institute of Physics, Helsinki, Finland
S. Czellar, J. Härkönen, A. Heikkinen, V. Karimäki, R. Kinnunen, M.J. Kortelainen, T. Lampén, K. Lassila-Perini, S. Lehti, T. Lindén, P. Luukka, T. Mäenpää, T. Peltola, E. Tuominen, J. Tuominiemi, E. Tuovinen, D. Ungaro, L. Wendland

Lappeenranta University of Technology, Lappeenranta, Finland
K. Banzuzi, A. Korpela, T. Tuuva

Laboratoire d'Annecy-le-Vieux de Physique des Particules, IN2P3-CNRS, Annecy-le-Vieux, France
D. Sillou

DSM/IRFU, CEA/Saclay, Gif-sur-Yvette, France
M. Besancon, S. Choudhury, M. Dejardin, D. Denegri, B. Fabbro, J.L. Faure, F. Ferri, S. Ganjour, A. Givernaud, P. Gras, G. Hamel de Monchenault, P. Jarry, E. Locci, J. Malcles, M. Marionneau, L. Millischer, J. Rander, A. Rosowsky, I. Shreyber, M. Titov

Laboratoire Leprince-Ringuet, Ecole Polytechnique, IN2P3-CNRS, Palaiseau, France
S. Baffioni, F. Beaudette, L. Benhabib, L. Bianchini, M. Bluj[11], C. Broutin, P. Busson, C. Charlot, N. Daci, T. Dahms, L. Dobrzynski, S. Elgammal, R. Granier de Cassagnac, M. Haguenauer, P. Miné, C. Mironov, C. Ochando, P. Paganini, D. Sabes, R. Salerno, Y. Sirois, C. Thiebaux, C. Veelken, A. Zabi

Institut Pluridisciplinaire Hubert Curien, Université de Strasbourg, Université de Haute Alsace Mulhouse, CNRS/IN2P3, Strasbourg, France
J.-L. Agram[12], J. Andrea, D. Bloch, D. Bodin, J.-M. Brom, M. Cardaci, E.C. Chabert, C. Collard, E. Conte[12], F. Drouhin[12], C. Ferro, J.-C. Fontaine[12], D. Gelé, U. Goerlach, S. Greder, P. Juillot, M. Karim[12], A.-C. Le Bihan, P. Van Hove

Centre de Calcul de l'Institut National de Physique Nucleaire et de Physique des Particules (IN2P3), Villeurbanne, France
F. Fassi, D. Mercier

Université de Lyon, Université Claude Bernard Lyon 1, CNRS-IN2P3, Institut de Physique Nucléaire de Lyon, Villeurbanne, France
C. Baty, S. Beauceron, N. Beaupere, M. Bedjidian, O. Bondu, G. Boudoul, D. Boumediene, H. Brun, J. Chasserat, R. Chierici[1], D. Contardo, P. Depasse, H. El Mamouni, A. Falkiewicz, J. Fay, S. Gascon, M. Gouzevitch, B. Ille, T. Kurca, T. Le Grand, M. Lethuillier, L. Mirabito, S. Perries, V. Sordini, S. Tosi, Y. Tschudi, P. Verdier, S. Viret

Institute of High Energy Physics and Informatization, Tbilisi State University, Tbilisi, Georgia
D. Lomidze

RWTH Aachen University, I. Physikalisches Institut, Aachen, Germany
G. Anagnostou, S. Beranek, M. Edelhoff, L. Feld, N. Heracleous, O. Hindrichs, R. Jussen, K. Klein, J. Merz, A. Ostapchuk, A. Perieanu, F. Raupach, J. Sammet, S. Schael, D. Sprenger, H. Weber, B. Wittmer, V. Zhukov[13]

RWTH Aachen University, III. Physikalisches Institut A, Aachen, Germany
M. Ata, E. Dietz-Laursonn, M. Erdmann, A. Güth, T. Hebbeker, C. Heidemann, K. Hoepfner, T. Klimkovich, D. Klingebiel, P. Kreuzer, D. Lanske[†], J. Lingemann, C. Magass, M. Merschmeyer, A. Meyer, M. Olschewski, P. Papacz, H. Pieta, H. Reithler, S.A. Schmitz, L. Sonnenschein, J. Steggemann, D. Teyssier, M. Weber

RWTH Aachen University, III. Physikalisches Institut B, Aachen, Germany
M. Bontenackels, V. Cherepanov, M. Davids, G. Flügge, H. Geenen, M. Geisler, W. Haj Ahmad, F. Hoehle, B. Kargoll, T. Kress, Y. Kuessel, A. Linn, A. Nowack, L. Perchalla, O. Pooth, J. Rennefeld, P. Sauerland, A. Stahl, D. Tornier, M.H. Zoeller

Deutsches Elektronen-Synchrotron, Hamburg, Germany
M. Aldaya Martin, W. Behrenhoff, U. Behrens, M. Bergholz[14], A. Bethani, K. Borras, A. Cakir, A. Campbell, E. Castro, D. Dammann, G. Eckerlin, D. Eckstein, A. Flossdorf, G. Flucke, A. Geiser, J. Hauk, H. Jung[1], M. Kasemann, P. Katsas, C. Kleinwort, H. Kluge, A. Knutsson, M. Krämer, D. Krücker, E. Kuznetsova, W. Lange, W. Lohmann[14], B. Lutz, R. Mankel, I. Marfin, M. Marienfeld, I.-A. Melzer-Pellmann, A.B. Meyer, J. Mnich, A. Mussgiller, S. Naumann-Emme, J. Olzem, A. Petrukhin, D. Pitzl, A. Raspereza, P.M. Ribeiro Cipriano, M. Rosin, J. Salfeld-Nebgen, R. Schmidt[14], T. Schoerner-Sadenius, N. Sen, A. Spiridonov, M. Stein, J. Tomaszewska, R. Walsh, C. Wissing

University of Hamburg, Hamburg, Germany
C. Autermann, V. Blobel, S. Bobrovskyi, J. Draeger, H. Enderle, U. Gebbert, M. Görner, T. Hermanns, K. Kaschube, G. Kaussen, H. Kirschenmann, R. Klanner, J. Lange, B. Mura, F. Nowak, N. Pietsch, C. Sander, H. Schettler, P. Schleper, E. Schlieckau, M. Schröder, T. Schum, H. Stadie, G. Steinbrück, J. Thomsen

Institut für Experimentelle Kernphysik, Karlsruhe, Germany
C. Barth, J. Berger, T. Chwalek, W. De Boer, A. Dierlamm, G. Dirkes, M. Feindt, J. Gruschke, M. Guthoff[1], C. Hackstein, F. Hartmann, M. Heinrich, H. Held, K.H. Hoffmann, S. Honc, I. Katkov[13], J.R. Komaragiri, T. Kuhr, D. Martschei, S. Mueller, Th. Müller, M. Niegel, O. Oberst, A. Oehler, J. Ott, T. Peiffer, G. Quast, K. Rabbertz, F. Ratnikov, N. Ratnikova, M. Renz, S. Röcker, C. Saout, A. Scheurer, P. Schieferdecker, F.-P. Schilling, M. Schmanau, G. Schott, H.J. Simonis, F.M. Stober, D. Troendle, J. Wagner-Kuhr, T. Weiler, M. Zeise, E.B. Ziebarth

Institute of Nuclear Physics "Demokritos", Aghia Paraskevi, Greece
G. Daskalakis, T. Geralis, S. Kesisoglou, A. Kyriakis, D. Loukas, I. Manolakos, A. Markou, C. Markou, C. Mavrommatis, E. Ntomari, E. Petrakou

University of Athens, Athens, Greece
L. Gouskos, T.J. Mertzimekis, A. Panagiotou, N. Saoulidou, E. Stiliaris

University of Ioánnina, Ioánnina, Greece
I. Evangelou, C. Foudas[1], P. Kokkas, N. Manthos, I. Papadopoulos, V. Patras, F.A. Triantis

KFKI Research Institute for Particle and Nuclear Physics, Budapest, Hungary
A. Aranyi, G. Bencze, L. Boldizsar, C. Hajdu[1], P. Hidas, D. Horvath[15], A. Kapusi, K. Krajczar[16], F. Sikler[1], G. Vesztergombi[16]

Institute of Nuclear Research ATOMKI, Debrecen, Hungary
N. Beni, J. Molnar, J. Palinkas, Z. Szillasi, V. Veszpremi

University of Debrecen, Debrecen, Hungary
J. Karancsi, P. Raics, Z.L. Trocsanyi, B. Ujvari

Panjab University, Chandigarh, India
S.B. Beri, V. Bhatnagar, N. Dhingra, R. Gupta, M. Jindal, M. Kaur, J.M. Kohli, M.Z. Mehta, N. Nishu, L.K. Saini, A. Sharma, A.P. Singh, J. Singh, S.P. Singh

University of Delhi, Delhi, India
S. Ahuja, B.C. Choudhary, A. Kumar, A. Kumar, S. Malhotra, M. Naimuddin, K. Ranjan, V. Sharma, R.K. Shivpuri

Saha Institute of Nuclear Physics, Kolkata, India
S. Banerjee, S. Bhattacharya, S. Dutta, B. Gomber, S. Jain, S. Jain, R. Khurana, S. Sarkar

Bhabha Atomic Research Centre, Mumbai, India
R.K. Choudhury, D. Dutta, S. Kailas, V. Kumar, A.K. Mohanty[1], L.M. Pant, P. Shukla

Tata Institute of Fundamental Research-EHEP, Mumbai, India
T. Aziz, S. Ganguly, M. Guchait[17], A. Gurtu[18], M. Maity[19], D. Majumder, G. Majumder, K. Mazumdar, G.B. Mohanty, B. Parida, A. Saha, K. Sudhakar, N. Wickramage

Tata Institute of Fundamental Research-HECR, Mumbai, India
S. Banerjee, S. Dugad, N.K. Mondal

Institute for Research in Fundamental Sciences (IPM), Tehran, Iran
H. Arfaei, H. Bakhshiansohi[20], S.M. Etesami[21], A. Fahim[20], M. Hashemi, H. Hesari, A. Jafari[20], M. Khakzad, A. Mohammadi[22], M. Mohammadi Najafabadi, S. Paktinat Mehdiabadi, B. Safarzadeh[23], M. Zeinali[21]

INFN Sezione di Bari[a], Università di Bari[b], Politecnico di Bari[c], Bari, Italy
M. Abbrescia[a,b], L. Barbone[a,b], C. Calabria[a,b], S.S. Chhibra[a,b], A. Colaleo[a], D. Creanza[a,c], N. De Filippis[a,c,1], M. De Palma[a,b], L. Fiore[a], G. Iaselli[a,c], L. Lusito[a,b], G. Maggi[a,c], M. Maggi[a], N. Manna[a,b], B. Marangelli[a,b], S. My[a,c], S. Nuzzo[a,b], N. Pacifico[a,b], A. Pompili[a,b], G. Pugliese[a,c], F. Romano[a,c], G. Selvaggi[a,b], L. Silvestris[a], G. Singh[a,b], S. Tupputi[a,b], G. Zito[a]

INFN Sezione di Bologna[a], Università di Bologna[b], Bologna, Italy
G. Abbiendi[a], A.C. Benvenuti[a], D. Bonacorsi[a], S. Braibant-Giacomelli[a,b], L. Brigliadori[a], P. Capiluppi[a,b], A. Castro[a,b], F.R. Cavallo[a], M. Cuffiani[a,b], G.M. Dallavalle[a], F. Fabbri[a], A. Fanfani[a,b], D. Fasanella[a,1], P. Giacomelli[a], C. Grandi[a], S. Marcellini[a], G. Masetti[a], M. Meneghelli[a,b], A. Montanari[a], F.L. Navarria[a,b], F. Odorici[a], A. Perrotta[a], F. Primavera[a], A.M. Rossi[a,b], T. Rovelli[a,b], G. Siroli[a,b], R. Travaglini[a,b]

INFN Sezione di Catania[a], Università di Catania[b], Catania, Italy
S. Albergo[a,b], G. Cappello[a,b], M. Chiorboli[a,b], S. Costa[a,b], R. Potenza[a,b], A. Tricomi[a,b], C. Tuve[a,b]

INFN Sezione di Firenze[a], Università di Firenze[b], Firenze, Italy
G. Barbagli[a], V. Ciulli[a,b], C. Civinini[a], R. D'Alessandro[a,b], E. Focardi[a,b], S. Frosali[a,b], E. Gallo[a], S. Gonzi[a,b], M. Meschini[a], S. Paoletti[a], G. Sguazzoni[a], A. Tropiano[a,1]

INFN Laboratori Nazionali di Frascati, Frascati, Italy
L. Benussi, S. Bianco, S. Colafranceschi[24], F. Fabbri, D. Piccolo

INFN Sezione di Genova, Genova, Italy
P. Fabbricatore, R. Musenich

INFN Sezione di Milano-Bicocca[a], Università di Milano-Bicocca[b], Milano, Italy
A. Benaglia[a,b,1], F. De Guio[a,b], L. Di Matteo[a,b], S. Gennai[a,1], A. Ghezzi[a,b], S. Malvezzi[a], A. Martelli[a,b], A. Massironi[a,b,1], D. Menasce[a], L. Moroni[a], M. Paganoni[a,b], D. Pedrini[a], S. Ragazzi[a,b], N. Redaelli[a], S. Sala[a], T. Tabarelli de Fatis[a,b]

INFN Sezione di Napoli[a], Università di Napoli "Federico II"[b], Napoli, Italy
S. Buontempo[a], C.A. Carrillo Montoya[a,1], N. Cavallo[a,25], A. De Cosa[a,b], O. Dogangun[a,b], F. Fabozzi[a,25], A.O.M. Iorio[a,1], L. Lista[a], M. Merola[a,b], P. Paolucci[a]

INFN Sezione di Padova[a], Università di Padova[b], Università di Trento (Trento)[c], Padova, Italy
P. Azzi[a], N. Bacchetta[a,1], P. Bellan[a,b], D. Bisello[a,b], A. Branca[a], R. Carlin[a,b], P. Checchia[a], T. Dorigo[a], U. Dosselli[a], F. Fanzago[a], F. Gasparini[a,b], U. Gasparini[a,b], A. Gozzelino[a], S. Lacaprara[a,26], I. Lazzizzera[a,c], M. Margoni[a,b], M. Mazzucato[a], A.T. Meneguzzo[a,b], M. Nespolo[a,1], L. Perrozzi[a], N. Pozzobon[a,b], P. Ronchese[a,b], F. Simonetto[a,b], E. Torassa[a], M. Tosi[a,b,1], S. Vanini[a,b], P. Zotto[a,b], G. Zumerle[a,b]

INFN Sezione di Pavia[a], Università di Pavia[b], Pavia, Italy
P. Baesso[a,b], U. Berzano[a], S.P. Ratti[a,b], C. Riccardi[a,b], P. Torre[a,b], P. Vitulo[a,b], C. Viviani[a,b]

INFN Sezione di Perugia[a], Università di Perugia[b], Perugia, Italy
M. Biasini[a,b], G.M. Bilei[a], B. Caponeri[a,b], L. Fanò[a,b], P. Lariccia[a,b], A. Lucaroni[a,b,1], G. Mantovani[a,b], M. Menichelli[a], A. Nappi[a,b], F. Romeo[a,b], A. Santocchia[a,b], S. Taroni[a,b,1], M. Valdata[a,b]

INFN Sezione di Pisa[a], Università di Pisa[b], Scuola Normale Superiore di Pisa[c], Pisa, Italy
P. Azzurri[a,c], G. Bagliesi[a], T. Boccali[a], G. Broccolo[a,c], R. Castaldi[a], R.T. D'Agnolo[a,c], R. Dell'Orso[a], F. Fiori[a,b], L. Foà[a,c], A. Giassi[a], A. Kraan[a], F. Ligabue[a,c], T. Lomtadze[a], L. Martini[a,27], A. Messineo[a,b], F. Palla[a], F. Palmonari[a], A. Rizzi[a], G. Segneri[a], A.T. Serban[a], P. Spagnolo[a], R. Tenchini[a], G. Tonelli[a,b,1], A. Venturi[a,1], P.G. Verdini[a]

INFN Sezione di Roma[a], Università di Roma "La Sapienza"[b], Roma, Italy
L. Barone[a,b], F. Cavallari[a], D. Del Re[a,b,1], M. Diemoz[a], C. Fanelli[a], D. Franci[a,b], M. Grassi[a,1], E. Longo[a,b], P. Meridiani[a], F. Micheli[a], S. Nourbakhsh[a], G. Organtini[a,b], F. Pandolfi[a,b], R. Paramatti[a], S. Rahatlou[a,b], M. Sigamani[a], L. Soffi[a]

INFN Sezione di Torino[a], Università di Torino[b], Università del Piemonte Orientale (Novara)[c], Torino, Italy
N. Amapane[a,b], R. Arcidiacono[a,c], S. Argiro[a,b], M. Arneodo[a,c], C. Biino[a], C. Botta[a,b], N. Cartiglia[a], R. Castello[a,b], M. Costa[a,b], N. Demaria[a], A. Graziano[a,b], C. Mariotti[a,1], S. Maselli[a], E. Migliore[a,b], V. Monaco[a,b], M. Musich[a], M.M. Obertino[a,c], N. Pastrone[a], M. Pelliccioni[a], A. Potenza[a,b], A. Romero[a,b], M. Ruspa[a,c], R. Sacchi[a,b], V. Sola[a,b], A. Solano[a,b], A. Staiano[a], A. Vilela Pereira[a]

INFN Sezione di Trieste[a], Università di Trieste[b], Trieste, Italy
S. Belforte[a], F. Cossutti[a], G. Della Ricca[a,b], B. Gobbo[a], M. Marone[a,b], D. Montanino[a,b,1], A. Penzo[a]

Kangwon National University, Chunchon, Korea
S.G. Heo, S.K. Nam

Kyungpook National University, Daegu, Korea
S. Chang, J. Chung, D.H. Kim, G.N. Kim, J.E. Kim, D.J. Kong, H. Park, S.R. Ro, D.C. Son

Chonnam National University, Institute for Universe and Elementary Particles, Kwangju, Korea
J.Y. Kim, Z.J. Kim, S. Song

Konkuk University, Seoul, Korea
H.Y. Jo

Korea University, Seoul, Korea
S. Choi, D. Gyun, B. Hong, M. Jo, H. Kim, T.J. Kim, K.S. Lee, D.H. Moon, S.K. Park, E. Seo, K.S. Sim

University of Seoul, Seoul, Korea
M. Choi, S. Kang, H. Kim, J.H. Kim, C. Park, I.C. Park, S. Park, G. Ryu

Sungkyunkwan University, Suwon, Korea
Y. Cho, Y. Choi, Y.K. Choi, J. Goh, M.S. Kim, B. Lee, J. Lee, S. Lee, H. Seo, I. Yu

Vilnius University, Vilnius, Lithuania
M.J. Bilinskas, I. Grigelionis, M. Janulis, D. Martisiute, P. Petrov, M. Polujanskas, T. Sabonis

Centro de Investigacion y de Estudios Avanzados del IPN, Mexico City, Mexico
H. Castilla-Valdez, E. De La Cruz-Burelo, I. Heredia-de La Cruz, R. Lopez-Fernandez, R. Magaña Villalba, J. Martínez-Ortega, A. Sánchez-Hernández, L.M. Villasenor-Cendejas

Universidad Iberoamericana, Mexico City, Mexico
S. Carrillo Moreno, F. Vazquez Valencia

Benemerita Universidad Autonoma de Puebla, Puebla, Mexico
H.A. Salazar Ibarguen

Universidad Autónoma de San Luis Potosí, San Luis Potosí, Mexico
E. Casimiro Linares, A. Morelos Pineda, M.A. Reyes-Santos

University of Auckland, Auckland, New Zealand
D. Krofcheck

University of Canterbury, Christchurch, New Zealand
A.J. Bell, P.H. Butler, R. Doesburg, S. Reucroft, H. Silverwood

National Centre for Physics, Quaid-I-Azam University, Islamabad, Pakistan
M. Ahmad, M.I. Asghar, H.R. Hoorani, S. Khalid, W.A. Khan, T. Khurshid, S. Qazi, M.A. Shah, M. Shoaib

Institute of Experimental Physics, Faculty of Physics, University of Warsaw, Warsaw, Poland
G. Brona, M. Cwiok, W. Dominik, K. Doroba, A. Kalinowski, M. Konecki, J. Krolikowski

Soltan Institute for Nuclear Studies, Warsaw, Poland
H. Bialkowska, B. Boimska, T. Frueboes, R. Gokieli, M. Górski, M. Kazana, K. Nawrocki, K. Romanowska-Rybinska, M. Szleper, G. Wrochna, P. Zalewski

Laboratório de Instrumentação e Física Experimental de Partículas, Lisboa, Portugal
N. Almeida, P. Bargassa, A. David, P. Faccioli, P.G. Ferreira Parracho, M. Gallinaro, P. Musella, A. Nayak, J. Pela[1], P.Q. Ribeiro, J. Seixas, J. Varela, P. Vischia

Joint Institute for Nuclear Research, Dubna, Russia
S. Afanasiev, I. Belotelov, P. Bunin, M. Gavrilenko, I. Golutvin, I. Gorbunov, A. Kamenev, V. Karjavin, G. Kozlov, A. Lanev, P. Moisenz, V. Palichik, V. Perelygin, S. Shmatov, V. Smirnov, A. Volodko, A. Zarubin

Petersburg Nuclear Physics Institute, Gatchina (St Petersburg), Russia
S. Evstyukhin, V. Golovtsov, Y. Ivanov, V. Kim, P. Levchenko, V. Murzin, V. Oreshkin, I. Smirnov, V. Sulimov, L. Uvarov, S. Vavilov, A. Vorobyev, An. Vorobyev

Institute for Nuclear Research, Moscow, Russia
Yu. Andreev, A. Dermenev, S. Gninenko, N. Golubev, M. Kirsanov, N. Krasnikov, V. Matveev, A. Pashenkov, A. Toropin, S. Troitsky

Institute for Theoretical and Experimental Physics, Moscow, Russia
V. Epshteyn, M. Erofeeva, V. Gavrilov, M. Kossov[1], A. Krokhotin, N. Lychkovskaya, V. Popov, G. Safronov, S. Semenov, V. Stolin, E. Vlasov, A. Zhokin

Moscow State University, Moscow, Russia
A. Belyaev, E. Boos, A. Ershov, A. Gribushin, O. Kodolova, V. Korotkikh, I. Lokhtin, A. Markina, S. Obraztsov, M. Perfilov, S. Petrushanko, L. Sarycheva, V. Savrin, A. Snigirev, I. Vardanyan

P.N. Lebedev Physical Institute, Moscow, Russia
V. Andreev, M. Azarkin, I. Dremin, M. Kirakosyan, A. Leonidov, G. Mesyats, S.V. Rusakov, A. Vinogradov

State Research Center of Russian Federation, Institute for High Energy Physics, Protvino, Russia
I. Azhgirey, I. Bayshev, S. Bitioukov, V. Grishin[1], V. Kachanov, D. Konstantinov, A. Korablev, V. Krychkine, V. Petrov, R. Ryutin, A. Sobol, L. Tourtchanovitch, S. Troshin, N. Tyurin, A. Uzunian, A. Volkov

University of Belgrade, Faculty of Physics and Vinca Institute of Nuclear Sciences, Belgrade, Serbia
P. Adzic[28], M. Djordjevic, M. Ekmedzic, D. Krpic[28], J. Milosevic

Centro de Investigaciones Energéticas Medioambientales y Tecnológicas (CIEMAT), Madrid, Spain
M. Aguilar-Benitez, J. Alcaraz Maestre, P. Arce, C. Battilana, E. Calvo, M. Cerrada, M. Chamizo Llatas, N. Colino, B. De La Cruz, A. Delgado Peris, C. Diez Pardos, D. Domínguez Vázquez, C. Fernandez Bedoya, J.P. Fernández Ramos, A. Ferrando, J. Flix, M.C. Fouz, P. Garcia-Abia, O. Gonzalez Lopez, S. Goy Lopez, J.M. Hernandez, M.I. Josa, G. Merino, J. Puerta Pelayo, I. Redondo, L. Romero, J. Santaolalla, M.S. Soares, C. Willmott

Universidad Autónoma de Madrid, Madrid, Spain
C. Albajar, G. Codispoti, J.F. de Trocóniz

Universidad de Oviedo, Oviedo, Spain
J. Cuevas, J. Fernandez Menendez, S. Folgueras, I. Gonzalez Caballero, L. Lloret Iglesias, J.M. Vizan Garcia

Instituto de Física de Cantabria (IFCA), CSIC-Universidad de Cantabria, Santander, Spain
J.A. Brochero Cifuentes, I.J. Cabrillo, A. Calderon, S.H. Chuang, J. Duarte Campderros, M. Felcini[29], M. Fernandez, G. Gomez, J. Gonzalez Sanchez, C. Jorda, P. Lobelle Pardo, A. Lopez Virto, J. Marco, R. Marco, C. Martinez Rivero, F. Matorras, F.J. Munoz Sanchez, J. Piedra Gomez[30], T. Rodrigo, A.Y. Rodríguez-Marrero, A. Ruiz-Jimeno, L. Scodellaro, M. Sobron Sanudo, I. Vila, R. Vilar Cortabitarte

CERN, European Organization for Nuclear Research, Geneva, Switzerland
D. Abbaneo, E. Auffray, G. Auzinger, P. Baillon, A.H. Ball, D. Barney, C. Bernet[5], W. Bialas, G. Bianchi, P. Bloch, A. Bocci, H. Breuker, K. Bunkowski, T. Camporesi, G. Cerminara, T. Christiansen, J.A. Coarasa Perez, B. Curé, D. D'Enterria, A. De Roeck, S. Di Guida, M. Dobson, N. Dupont-Sagorin, A. Elliott-Peisert, B. Frisch, W. Funk, A. Gaddi, G. Georgiou, H. Gerwig, M. Giffels, D. Gigi, K. Gill, D. Giordano, M. Giunta, F. Glege, R. Gomez-Reino Garrido, P. Govoni, S. Gowdy, R. Guida, L. Guiducci, M. Hansen, C. Hartl, J. Harvey, B. Hegner, A. Hinzmann, H.F. Hoffmann, V. Innocente, P. Janot, K. Kaadze, E. Karavakis, K. Kousouris, P. Lecoq, P. Lenzi, C. Lourenço, T. Mäki, M. Malberti, L. Malgeri, M. Mannelli, L. Masetti, G. Mavromanolakis, F. Meijers, S. Mersi, E. Meschi, R. Moser, M.U. Mozer, M. Mulders, E. Nesvold, M. Nguyen, T. Orimoto, L. Orsini, E. Palencia Cortezon, E. Perez, A. Petrilli, A. Pfeiffer, M. Pierini, M. Pimiä, D. Piparo, G. Polese, L. Quertenmont, A. Racz, W. Reece, J. Rodrigues Antunes, G. Rolandi[31], T. Rommerskirchen, C. Rovelli[32], M. Rovere, H. Sakulin, F. Santanastasio, C. Schäfer, C. Schwick, I. Segoni, A. Sharma, P. Siegrist, P. Silva, M. Simon, P. Sphicas[33], D. Spiga, M. Spiropulu[4], M. Stoye, A. Tsirou, G.I. Veres[16], P. Vichoudis, H.K. Wöhri, S.D. Worm[34], W.D. Zeuner

Paul Scherrer Institut, Villigen, Switzerland
W. Bertl, K. Deiters, W. Erdmann, K. Gabathuler, R. Horisberger, Q. Ingram, H.C. Kaestli, S. König, D. Kotlinski, U. Langenegger, F. Meier, D. Renker, T. Rohe, J. Sibille[35]

Institute for Particle Physics, ETH Zurich, Zurich, Switzerland
L. Bäni, P. Bortignon, M.A. Buchmann, B. Casal, N. Chanon, Z. Chen, A. Deisher, G. Dissertori, M. Dittmar, M. Dünser, J. Eugster, K. Freudenreich, C. Grab, P. Lecomte, W. Lustermann, P. Martinez Ruiz del Arbol, N. Mohr, F. Moortgat, C. Nägeli[36], P. Nef, F. Nessi-Tedaldi, L. Pape, F. Pauss, M. Peruzzi, F.J. Ronga, M. Rossini, L. Sala, A.K. Sanchez, M.-C. Sawley, A. Starodumov[37], B. Stieger, M. Takahashi, L. Tauscher[†], A. Thea, K. Theofilatos, D. Treille, C. Urscheler, R. Wallny, H.A. Weber, L. Wehrli, J. Weng

Universität Zürich, Zurich, Switzerland
E. Aguilo, C. Amsler, V. Chiochia, S. De Visscher, C. Favaro, M. Ivova Rikova, B. Millan Mejias, P. Otiougova, P. Robmann, A. Schmidt, H. Snoek, M. Verzetti

National Central University, Chung-Li, Taiwan
Y.H. Chang, K.H. Chen, C.M. Kuo, S.W. Li, W. Lin, Z.K. Liu, Y.J. Lu, D. Mekterovic, R. Volpe, S.S. Yu

National Taiwan University (NTU), Taipei, Taiwan
P. Bartalini, P. Chang, Y.H. Chang, Y.W. Chang, Y. Chao, K.F. Chen, C. Dietz, U. Grundler, W.-S. Hou, Y. Hsiung, K.Y. Kao, Y.J. Lei, R.-S. Lu, X. Shi, J.G. Shiu, Y.M. Tzeng, X. Wan, M. Wang

Cukurova University, Adana, Turkey
A. Adiguzel, M.N. Bakirci[38], S. Cerci[39], C. Dozen, I. Dumanoglu, E. Eskut, S. Girgis, G. Gokbulut, I. Hos, E.E. Kangal, G. Karapinar, A. Kayis Topaksu, G. Onengut, K. Ozdemir, S. Ozturk[40], A. Polatoz, K. Sogut[41], D. Sunar Cerci[39], B. Tali[39], H. Topakli[38], D. Uzun, L.N. Vergili, M. Vergili

Middle East Technical University, Physics Department, Ankara, Turkey
I.V. Akin, T. Aliev, B. Bilin, S. Bilmis, M. Deniz, H. Gamsizkan, A.M. Guler, K. Ocalan, A. Ozpineci, M. Serin, R. Sever, U.E. Surat, M. Yalvac, E. Yildirim, M. Zeyrek

Bogazici University, Istanbul, Turkey
M. Deliomeroglu, E. Gülmez, B. Isildak, M. Kaya[42], O. Kaya[42], S. Ozkorucuklu[43], N. Sonmez[44]

National Scientific Center, Kharkov Institute of Physics and Technology, Kharkov, Ukraine
L. Levchuk

University of Bristol, Bristol, United Kingdom
F. Bostock, J.J. Brooke, E. Clement, D. Cussans, H. Flacher, R. Frazier, J. Goldstein, M. Grimes, G.P. Heath, H.F. Heath, L. Kreczko, S. Metson, D.M. Newbold[34], K. Nirunpong, A. Poll, S. Senkin, V.J. Smith, T. Williams

Rutherford Appleton Laboratory, Didcot, United Kingdom
L. Basso[45], A. Belyaev[45], C. Brew, R.M. Brown, B. Camanzi, D.J.A. Cockerill, J.A. Coughlan, K. Harder, S. Harper, J. Jackson, B.W. Kennedy, E. Olaiya, D. Petyt, B.C. Radburn-Smith, C.H. Shepherd-Themistocleous, I.R. Tomalin, W.J. Womersley

Imperial College, London, United Kingdom
R. Bainbridge, G. Ball, R. Beuselinck, O. Buchmuller, D. Colling, N. Cripps, M. Cutajar, P. Dauncey, G. Davies, M. Della Negra, W. Ferguson, J. Fulcher, D. Futyan, A. Gilbert, A. Guneratne Bryer, G. Hall, Z. Hatherell, J. Hays, G. Iles, M. Jarvis, G. Karapostoli, L. Lyons, A.-M. Magnan, J. Marrouche, B. Mathias, R. Nandi, J. Nash, A. Nikitenko[37], A. Papageorgiou, M. Pesaresi, K. Petridis, M. Pioppi[46], D.M. Raymond, S. Rogerson, N. Rompotis, A. Rose, M.J. Ryan, C. Seez, P. Sharp, A. Sparrow, A. Tapper, S. Tourneur, M. Vazquez Acosta, T. Virdee, S. Wakefield, N. Wardle, D. Wardrope, T. Whyntie

Brunel University, Uxbridge, United Kingdom
M. Barrett, M. Chadwick, J.E. Cole, P.R. Hobson, A. Khan, P. Kyberd, D. Leslie, W. Martin, I.D. Reid, P. Symonds, L. Teodorescu, M. Turner

Baylor University, Waco, USA
K. Hatakeyama, H. Liu, T. Scarborough

The University of Alabama, Tuscaloosa, USA
C. Henderson

Boston University, Boston, USA
A. Avetisyan, T. Bose, E. Carrera Jarrin, C. Fantasia, A. Heister, J.St. John, P. Lawson, D. Lazic, J. Rohlf, D. Sperka, L. Sulak

Brown University, Providence, USA
S. Bhattacharya, D. Cutts, A. Ferapontov, U. Heintz, S. Jabeen, G. Kukartsev, G. Landsberg, M. Luk, M. Narain, D. Nguyen, M. Segala, T. Sinthuprasith, T. Speer, K.V. Tsang

University of California, Davis, Davis, USA
R. Breedon, G. Breto, M. Calderon De La Barca Sanchez, M. Caulfield, S. Chauhan, M. Chertok, J. Conway, R. Conway, P.T. Cox, J. Dolen, R. Erbacher, M. Gardner, R. Houtz, W. Ko, A. Kopecky, R. Lander, O. Mall, T. Miceli, R. Nelson, D. Pellett, J. Robles, B. Rutherford, M. Searle, J. Smith, M. Squires, M. Tripathi, R. Vasquez Sierra

University of California, Los Angeles, Los Angeles, USA
V. Andreev, K. Arisaka, D. Cline, R. Cousins, J. Duris, S. Erhan, P. Everaerts, C. Farrell, J. Hauser, M. Ignatenko, C. Jarvis, C. Plager, G. Rakness, P. Schlein[†], J. Tucker, V. Valuev, M. Weber

University of California, Riverside, Riverside, USA
J. Babb, R. Clare, J. Ellison, J.W. Gary, F. Giordano, G. Hanson, G.Y. Jeng, H. Liu, O.R. Long, A. Luthra, H. Nguyen, S. Paramesvaran, J. Sturdy, S. Sumowidagdo, R. Wilken, S. Wimpenny

University of California, San Diego, La Jolla, USA
W. Andrews, J.G. Branson, G.B. Cerati, S. Cittolin, D. Evans, F. Golf, A. Holzner, R. Kelley, M. Lebourgeois, J. Letts, I. Macneill, B. Mangano, S. Padhi, C. Palmer, G. Petrucciani, H. Pi, M. Pieri, R. Ranieri, M. Sani, I. Sfiligoi, V. Sharma, S. Simon, E. Sudano, M. Tadel, Y. Tu, A. Vartak, S. Wasserbaech[47], F. Würthwein, A. Yagil, J. Yoo

University of California, Santa Barbara, Santa Barbara, USA
D. Barge, R. Bellan, C. Campagnari, M. D'Alfonso, T. Danielson, K. Flowers, P. Geffert, C. George, J. Incandela, C. Justus, P. Kalavase, S.A. Koay, D. Kovalskyi[1], V. Krutelyov, S. Lowette, N. Mccoll, S.D. Mullin, V. Pavlunin, F. Rebassoo, J. Ribnik, J. Richman, R. Rossin, D. Stuart, W. To, J.R. Vlimant, C. West

California Institute of Technology, Pasadena, USA
A. Apresyan, A. Bornheim, J. Bunn, Y. Chen, E. Di Marco, J. Duarte, M. Gataullin, Y. Ma, A. Mott, H.B. Newman, C. Rogan, V. Timciuc, P. Traczyk, J. Veverka, R. Wilkinson, Y. Yang, R.Y. Zhu

Carnegie Mellon University, Pittsburgh, USA
B. Akgun, R. Carroll, T. Ferguson, Y. Iiyama, D.W. Jang, S.Y. Jun, Y.F. Liu, M. Paulini, J. Russ, H. Vogel, I. Vorobiev

University of Colorado at Boulder, Boulder, USA
J.P. Cumalat, M.E. Dinardo, B.R. Drell, C.J. Edelmaier, W.T. Ford, A. Gaz, B. Heyburn, E. Luiggi Lopez, U. Nauenberg, J.G. Smith, K. Stenson, K.A. Ulmer, S.R. Wagner, S.L. Zang

Cornell University, Ithaca, USA
L. Agostino, J. Alexander, A. Chatterjee, N. Eggert, L.K. Gibbons, B. Heltsley, W. Hopkins, A. Khukhunaishvili, B. Kreis, N. Mirman, G. Nicolas Kaufman, J.R. Patterson, D. Puigh, A. Ryd, E. Salvati, W. Sun, W.D. Teo, J. Thom, J. Thompson, J. Vaughan, Y. Weng, L. Winstrom, P. Wittich

Fairfield University, Fairfield, USA
A. Biselli, G. Cirino, D. Winn

Fermi National Accelerator Laboratory, Batavia, USA
S. Abdullin, M. Albrow, J. Anderson, G. Apollinari, M. Atac, J.A. Bakken, L.A.T. Bauerdick, A. Beretvas, J. Berryhill, P.C. Bhat, I. Bloch, K. Burkett, J.N. Butler, V. Chetluru, H.W.K. Cheung, F. Chlebana, S. Cihangir, W. Cooper, D.P. Eartly, V.D. Elvira, S. Esen, I. Fisk, J. Freeman, Y. Gao, E. Gottschalk, D. Green, O. Gutsche, J. Hanlon, R.M. Harris, J. Hirschauer, B. Hooberman, H. Jensen, S. Jindariani, M. Johnson, U. Joshi, B. Klima, S. Kunori, S. Kwan, C. Leonidopoulos, D. Lincoln, R. Lipton, J. Lykken, K. Maeshima, J.M. Marraffino, S. Maruyama, D. Mason, P. McBride, T. Miao, K. Mishra, S. Mrenna, Y. Musienko[48], C. Newman-Holmes, V. O'Dell, J. Pivarski, R. Pordes, O. Prokofyev, T. Schwarz, E. Sexton-Kennedy, S. Sharma, W.J. Spalding, L. Spiegel, P. Tan, L. Taylor, S. Tkaczyk, L. Uplegger, E.W. Vaandering, R. Vidal, J. Whitmore, W. Wu, F. Yang, F. Yumiceva, J.C. Yun

University of Florida, Gainesville, USA
D. Acosta, P. Avery, D. Bourilkov, M. Chen, S. Das, M. De Gruttola, G.P. Di Giovanni, D. Dobur, A. Drozdetskiy, R.D. Field, M. Fisher, Y. Fu, I.K. Furic, J. Gartner, S. Goldberg, J. Hugon, B. Kim, J. Konigsberg, A. Korytov, A. Kropivnitskaya, T. Kypreos, J.F. Low, K. Matchev, P. Milenovic[49], G. Mitselmakher, L. Muniz, M. Park, R. Remington, A. Rinkevicius, M. Schmitt, B. Scurlock, P. Sellers, N. Skhirtladze, M. Snowball, D. Wang, J. Yelton, M. Zakaria

Florida International University, Miami, USA
V. Gaultney, L.M. Lebolo, S. Linn, P. Markowitz, G. Martinez, J.L. Rodriguez

Florida State University, Tallahassee, USA
T. Adams, A. Askew, J. Bochenek, J. Chen, B. Diamond, S.V. Gleyzer, J. Haas, S. Hagopian, V. Hagopian, M. Jenkins, K.F. Johnson, H. Prosper, S. Sekmen, V. Veeraraghavan, M. Weinberg

Florida Institute of Technology, Melbourne, USA
M.M. Baarmand, B. Dorney, M. Hohlmann, H. Kalakhety, I. Vodopiyanov

University of Illinois at Chicago (UIC), Chicago, USA
M.R. Adams, I.M. Anghel, L. Apanasevich, Y. Bai, V.E. Bazterra, R.R. Betts, J. Callner, R. Cavanaugh, C. Dragoiu, L. Gauthier, C.E. Gerber, D.J. Hofman, S. Khalatyan, G.J. Kunde[50], F. Lacroix, M. Malek, C. O'Brien, C. Silkworth, C. Silvestre, D. Strom, N. Varelas

The University of Iowa, Iowa City, USA
U. Akgun, E.A. Albayrak, B. Bilki[51], W. Clarida, F. Duru, S. Griffiths, C.K. Lae, E. McCliment, J.-P. Merlo, H. Mermerkaya[52], A. Mestvirishvili, A. Moeller, J. Nachtman, C.R. Newsom, E. Norbeck, J. Olson, Y. Onel, F. Ozok, S. Sen, E. Tiras, J. Wetzel, T. Yetkin, K. Yi

Johns Hopkins University, Baltimore, USA
B.A. Barnett, B. Blumenfeld, S. Bolognesi, A. Bonato, C. Eskew, D. Fehling, G. Giurgiu, A.V. Gritsan, Z.J. Guo, G. Hu, P. Maksimovic, S. Rappoccio, M. Swartz, N.V. Tran, A. Whitbeck

The University of Kansas, Lawrence, USA
P. Baringer, A. Bean, G. Benelli, O. Grachov, R.P. Kenny Iii, M. Murray, D. Noonan, S. Sanders, R. Stringer, G. Tinti, J.S. Wood, V. Zhukova

Kansas State University, Manhattan, USA
A.F. Barfuss, T. Bolton, I. Chakaberia, A. Ivanov, S. Khalil, M. Makouski, Y. Maravin, S. Shrestha, I. Svintradze

Lawrence Livermore National Laboratory, Livermore, USA
J. Gronberg, D. Lange, D. Wright

University of Maryland, College Park, USA
A. Baden, M. Boutemeur, B. Calvert, S.C. Eno, J.A. Gomez, N.J. Hadley, R.G. Kellogg, M. Kirn, T. Kolberg, Y. Lu, A.C. Mignerey, A. Peterman, K. Rossato, P. Rumerio, A. Skuja, J. Temple, M.B. Tonjes, S.C. Tonwar, E. Twedt

Massachusetts Institute of Technology, Cambridge, USA
B. Alver, G. Bauer, J. Bendavid, W. Busza, E. Butz, I.A. Cali, M. Chan, V. Dutta, G. Gomez Ceballos, M. Goncharov, K.A. Hahn, P. Harris, Y. Kim, M. Klute, Y.-J. Lee, W. Li, P.D. Luckey, T. Ma, S. Nahn, C. Paus, D. Ralph, C. Roland, G. Roland, M. Rudolph, G.S.F. Stephans, F. Stöckli, K. Sumorok, K. Sung, D. Velicanu, E.A. Wenger, R. Wolf, B. Wyslouch, S. Xie, M. Yang, Y. Yilmaz, A.S. Yoon, M. Zanetti

University of Minnesota, Minneapolis, USA
S.I. Cooper, P. Cushman, B. Dahmes, A. De Benedetti, G. Franzoni, A. Gude, J. Haupt, S.C. Kao, K. Klapoetke, Y. Kubota, J. Mans, N. Pastika, V. Rekovic, R. Rusack, M. Sasseville, A. Singovsky, N. Tambe, J. Turkewitz

University of Mississippi, University, USA
L.M. Cremaldi, R. Godang, R. Kroeger, L. Perera, R. Rahmat, D.A. Sanders, D. Summers

University of Nebraska-Lincoln, Lincoln, USA
E. Avdeeva, K. Bloom, S. Bose, J. Butt, D.R. Claes, A. Dominguez, M. Eads, P. Jindal, J. Keller, I. Kravchenko, J. Lazo-Flores, H. Malbouisson, S. Malik, G.R. Snow

State University of New York at Buffalo, Buffalo, USA
U. Baur, A. Godshalk, I. Iashvili, S. Jain, A. Kharchilava, A. Kumar, S.P. Shipkowski, K. Smith, Z. Wan

Northeastern University, Boston, USA
G. Alverson, E. Barberis, D. Baumgartel, M. Chasco, D. Trocino, D. Wood, J. Zhang

Northwestern University, Evanston, USA
A. Anastassov, A. Kubik, N. Mucia, N. Odell, R.A. Ofierzynski, B. Pollack, A. Pozdnyakov, M. Schmitt, S. Stoynev, M. Velasco, S. Won

University of Notre Dame, Notre Dame, USA
L. Antonelli, D. Berry, A. Brinkerhoff, M. Hildreth, C. Jessop, D.J. Karmgard, J. Kolb, K. Lannon, W. Luo, S. Lynch, N. Marinelli, D.M. Morse, T. Pearson, R. Ruchti, J. Slaunwhite, N. Valls, M. Wayne, M. Wolf, J. Ziegler

The Ohio State University, Columbus, USA
B. Bylsma, L.S. Durkin, C. Hill, P. Killewald, K. Kotov, T.Y. Ling, M. Rodenburg, C. Vuosalo, G. Williams

Princeton University, Princeton, USA
N. Adam, E. Berry, P. Elmer, D. Gerbaudo, V. Halyo, P. Hebda, J. Hegeman, A. Hunt, E. Laird, D. Lopes Pegna, P. Lujan, D. Marlow, T. Medvedeva, M. Mooney, J. Olsen, P. Piroué, X. Quan, A. Raval, H. Saka, D. Stickland, C. Tully, J.S. Werner, A. Zuranski

University of Puerto Rico, Mayaguez, USA
J.G. Acosta, X.T. Huang, A. Lopez, H. Mendez, S. Oliveros, J.E. Ramirez Vargas, A. Zatserklyaniy

Purdue University, West Lafayette, USA
E. Alagoz, V.E. Barnes, D. Benedetti, G. Bolla, L. Borrello, D. Bortoletto, M. De Mattia, A. Everett, L. Gutay, Z. Hu, M. Jones, O. Koybasi, M. Kress, A.T. Laasanen, N. Leonardo, V. Maroussov, P. Merkel, D.H. Miller, N. Neumeister, I. Shipsey, D. Silvers, A. Svyatkovskiy, M. Vidal Marono, H.D. Yoo, J. Zablocki, Y. Zheng

Purdue University Calumet, Hammond, USA
S. Guragain, N. Parashar

Rice University, Houston, USA
A. Adair, C. Boulahouache, V. Cuplov, K.M. Ecklund, F.J.M. Geurts, B.P. Padley, R. Redjimi, J. Roberts, J. Zabel

University of Rochester, Rochester, USA
B. Betchart, A. Bodek, Y.S. Chung, R. Covarelli, P. de Barbaro, R. Demina, Y. Eshaq, A. Garcia-Bellido, P. Goldenzweig, Y. Gotra, J. Han, A. Harel, D.C. Miner, G. Petrillo, W. Sakumoto, D. Vishnevskiy, M. Zielinski

The Rockefeller University, New York, USA
A. Bhatti, R. Ciesielski, L. Demortier, K. Goulianos, G. Lungu, S. Malik, C. Mesropian

Rutgers, the State University of New Jersey, Piscataway, USA
S. Arora, O. Atramentov, A. Barker, J.P. Chou, C. Contreras-Campana, E. Contreras-Campana, D. Duggan, D. Ferencek, Y. Gershtein, R. Gray, E. Halkiadakis, D. Hidas, D. Hits, A. Lath, S. Panwalkar, M. Park, R. Patel, A. Richards, K. Rose, S. Salur, S. Schnetzer, S. Somalwar, R. Stone, S. Thomas

University of Tennessee, Knoxville, USA
G. Cerizza, M. Hollingsworth, S. Spanier, Z.C. Yang, A. York

Texas A&M University, College Station, USA
R. Eusebi, W. Flanagan, J. Gilmore, T. Kamon[53], V. Khotilovich, R. Montalvo, I. Osipenkov, Y. Pakhotin, A. Perloff, J. Roe, A. Safonov, T. Sakuma, S. Sengupta, I. Suarez, A. Tatarinov, D. Toback

Texas Tech University, Lubbock, USA
N. Akchurin, C. Bardak, J. Damgov, P.R. Dudero, C. Jeong, K. Kovitanggoon, S.W. Lee, T. Libeiro, P. Mane, Y. Roh, A. Sill, I. Volobouev, R. Wigmans, E. Yazgan

Vanderbilt University, Nashville, USA
E. Appelt, E. Brownson, D. Engh, C. Florez, W. Gabella, A. Gurrola, M. Issah, W. Johns, C. Johnston, P. Kurt, C. Maguire, A. Melo, P. Sheldon, B. Snook, S. Tuo, J. Velkovska

University of Virginia, Charlottesville, USA
M.W. Arenton, M. Balazs, S. Boutle, S. Conetti, B. Cox, B. Francis, S. Goadhouse, J. Goodell, R. Hirosky, A. Ledovskoy, C. Lin, C. Neu, J. Wood, R. Yohay

Wayne State University, Detroit, USA
S. Gollapinni, R. Harr, P.E. Karchin, C. Kottachchi Kankanamge Don, P. Lamichhane, M. Mattson, C. Milstène, A. Sakharov

University of Wisconsin, Madison, USA
M. Anderson, M. Bachtis, D. Belknap, J.N. Bellinger, J. Bernardini, D. Carlsmith, M. Cepeda, S. Dasu, J. Efron, E. Friis, L. Gray, K.S. Grogg, M. Grothe, R. Hall-Wilton, M. Herndon, A. Hervé, P. Klabbers, J. Klukas, A. Lanaro, C. Lazaridis, J. Leonard, R. Loveless, A. Mohapatra, I. Ojalvo, G.A. Pierro, I. Ross, A. Savin, W.H. Smith, J. Swanson

†: Deceased
1: Also at CERN, European Organization for Nuclear Research, Geneva, Switzerland
2: Also at National Institute of Chemical Physics and Biophysics, Tallinn, Estonia
3: Also at Universidade Federal do ABC, Santo Andre, Brazil
4: Also at California Institute of Technology, Pasadena, USA
5: Also at Laboratoire Leprince-Ringuet, Ecole Polytechnique, IN2P3-CNRS, Palaiseau, France
6: Also at Suez Canal University, Suez, Egypt
7: Also at Cairo University, Cairo, Egypt
8: Also at British University, Cairo, Egypt
9: Also at Fayoum University, El-Fayoum, Egypt

10: Also at Ain Shams University, Cairo, Egypt
11: Also at Soltan Institute for Nuclear Studies, Warsaw, Poland
12: Also at Université de Haute-Alsace, Mulhouse, France
13: Also at Moscow State University, Moscow, Russia
14: Also at Brandenburg University of Technology, Cottbus, Germany
15: Also at Institute of Nuclear Research ATOMKI, Debrecen, Hungary
16: Also at Eötvös Loránd University, Budapest, Hungary
17: Also at Tata Institute of Fundamental Research-HECR, Mumbai, India
18: Now at King Abdulaziz University, Jeddah, Saudi Arabia
19: Also at University of Visva-Bharati, Santiniketan, India
20: Also at Sharif University of Technology, Tehran, Iran
21: Also at Isfahan University of Technology, Isfahan, Iran
22: Also at Shiraz University, Shiraz, Iran
23: Also at Plasma Physics Research Center, Science and Research Branch, Islamic Azad University, Teheran, Iran
24: Also at Facoltà Ingegneria Università di Roma, Roma, Italy
25: Also at Università della Basilicata, Potenza, Italy
26: Also at Laboratori Nazionali di Legnaro dell'INFN, Legnaro, Italy
27: Also at Università degli studi di Siena, Siena, Italy
28: Also at Faculty of Physics of University of Belgrade, Belgrade, Serbia
29: Also at University of California, Los Angeles, Los Angeles, USA
30: Also at University of Florida, Gainesville, USA
31: Also at Scuola Normale e Sezione dell'INFN, Pisa, Italy
32: Also at INFN Sezione di Roma; Università di Roma "La Sapienza", Roma, Italy
33: Also at University of Athens, Athens, Greece
34: Also at Rutherford Appleton Laboratory, Didcot, United Kingdom
35: Also at The University of Kansas, Lawrence, USA
36: Also at Paul Scherrer Institut, Villigen, Switzerland
37: Also at Institute for Theoretical and Experimental Physics, Moscow, Russia
38: Also at Gaziosmanpasa University, Tokat, Turkey
39: Also at Adiyaman University, Adiyaman, Turkey
40: Also at The University of Iowa, Iowa City, USA
41: Also at Mersin University, Mersin, Turkey
42: Also at Kafkas University, Kars, Turkey
43: Also at Suleyman Demirel University, Isparta, Turkey
44: Also at Ege University, Izmir, Turkey
45: Also at School of Physics and Astronomy, University of Southampton, Southampton, United Kingdom
46: Also at INFN Sezione di Perugia; Università di Perugia, Perugia, Italy
47: Also at Utah Valley University, Orem, USA
48: Also at Institute for Nuclear Research, Moscow, Russia
49: Also at University of Belgrade, Faculty of Physics and Vinca Institute of Nuclear Sciences, Belgrade, Serbia
50: Also at Los Alamos National Laboratory, Los Alamos, USA
51: Also at Argonne National Laboratory, Argonne, USA
52: Also at Erzincan University, Erzincan, Turkey
53: Also at Kyungpook National University, Daegu, Korea